Molecular Architectures built from Heteroborane Clusters:

Electronic Structure and Beyond

Josep M. Oliva
Institute of Chemical-Physics, Spanish Research Council

Paris 2012 Workshop on ab initio Valence-Bond theory
July 2012

Three broad fields in Boron Chemistry

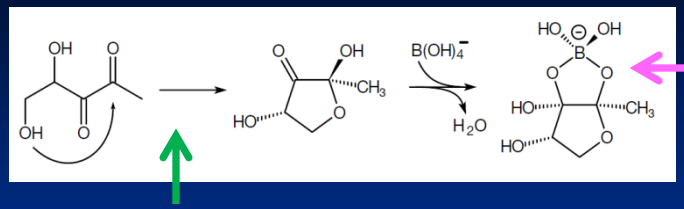

Autoinducer in cell-cell signaling

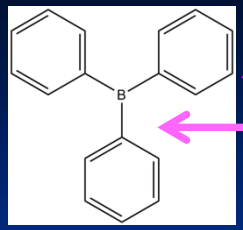

Triphenyl borane

1- (In)organic Chemistry with one ore few boron atoms as constitutent of molecules

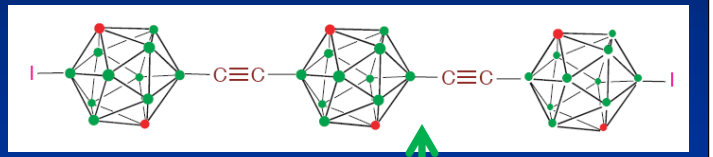

2 - Polyhedral Boron Chemistry

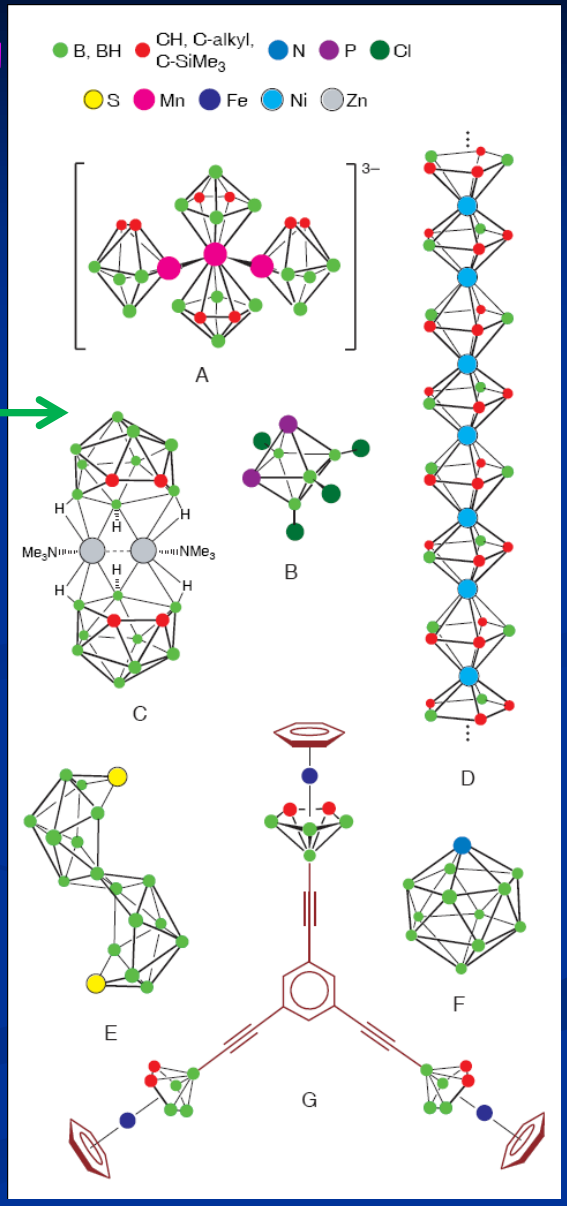

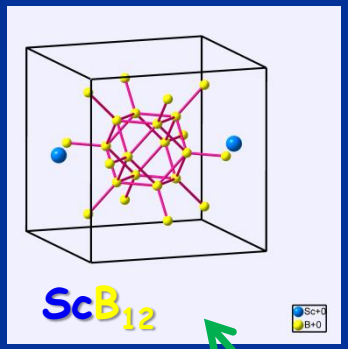

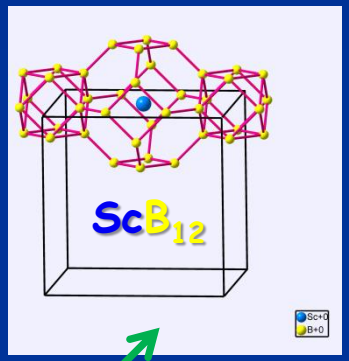

3 - Solid-State Boron Chemistry

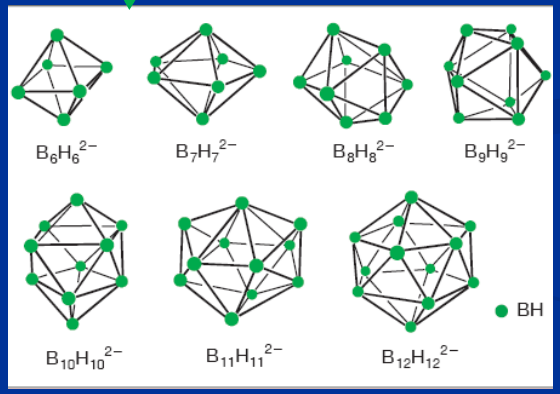

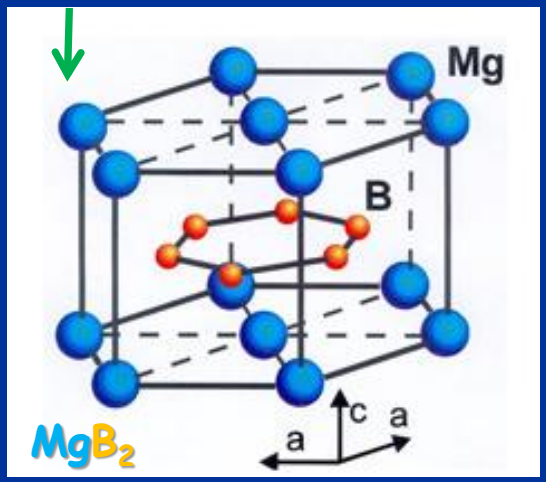

Common Motif

1D, 2D and 3D structural patterns of boron atoms

Context of the Scientific Problem

-This talk focusses mainly on electronic structure of polyhedral heteroboranes in combination with: themselves (nD), metals and biomolecules

- Polyhedral Boron chemistry has provided very rich molecular architectural constructs since the second half of XXth century and beginning of the XXIst century

- Scarce knowledge on electronic structure of Polyhedral Boron Chemistry and Solid-State Boron Chemistry

- Biological role for Boron unknown

Polyhedral Heteroborane Quantum Chemistry

Electronic Structure in Spin ≥ 0 one-, two- and three-Dimensional Architectural Constructs

Endohedral and Transition-Metal Complexes

Excited States

Experiments on Ion-Molecule Reactions

Electronic Structure as Function of Charge (q), Spin (S), Vertex/Cage Subtituents (R) and Wave-Function Nature (Ψ)

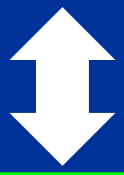

Valence-Bond Theoretic Approach $\leftrightarrow$ Composite-System Models

Electronic Structure/Geometry as Function of Substituent *R*

Neutral Icosahedral *ortho*-carboranes
$1,2\text{-}(R)_2\text{-}1,2\text{-}C_2B_{10}H_{10}$

C···*C* distance as function of substituent ***R***

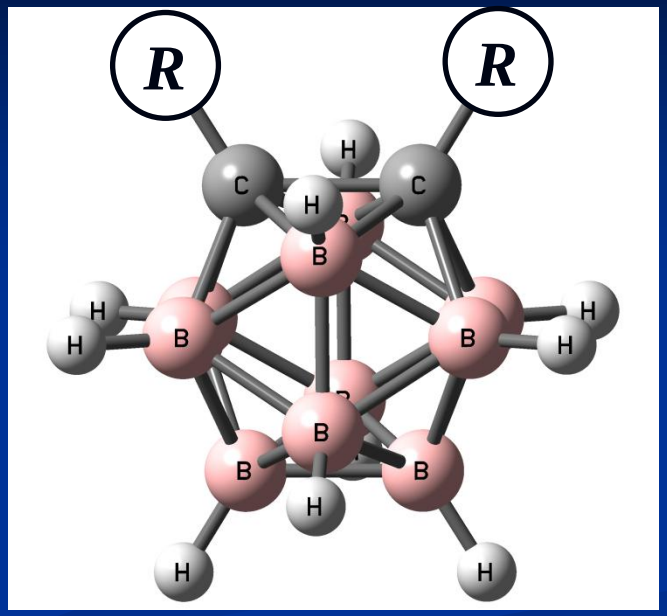

Dianions: *C*···*C* distance as function of substituent ***R***

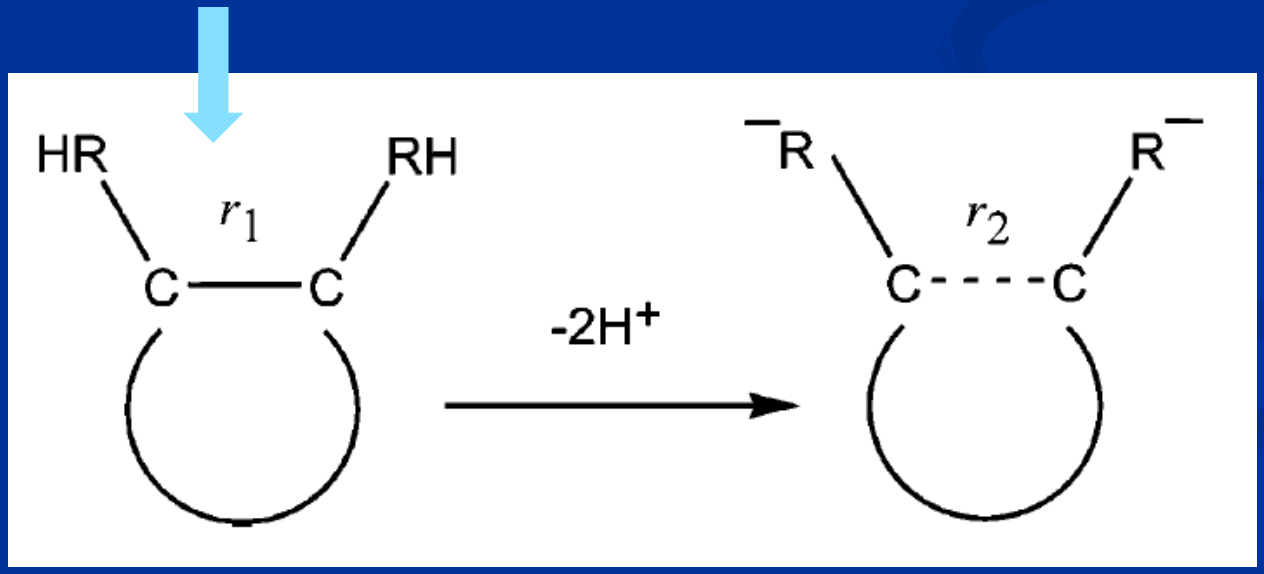

B3LYP/6-31G* optimized geometries

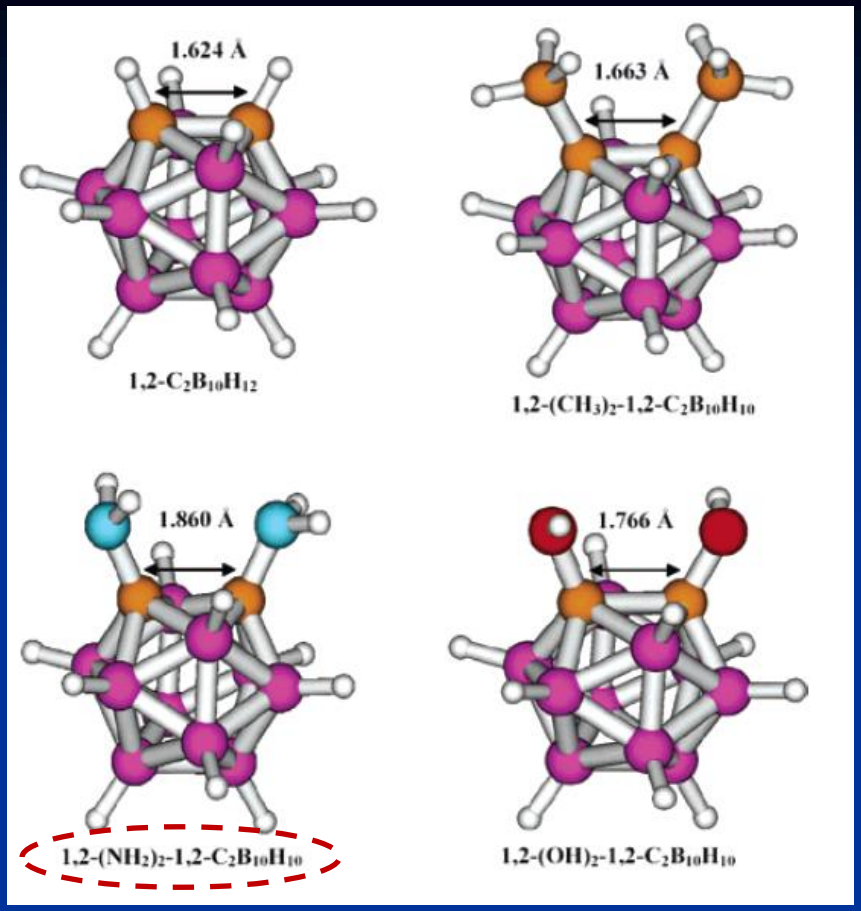

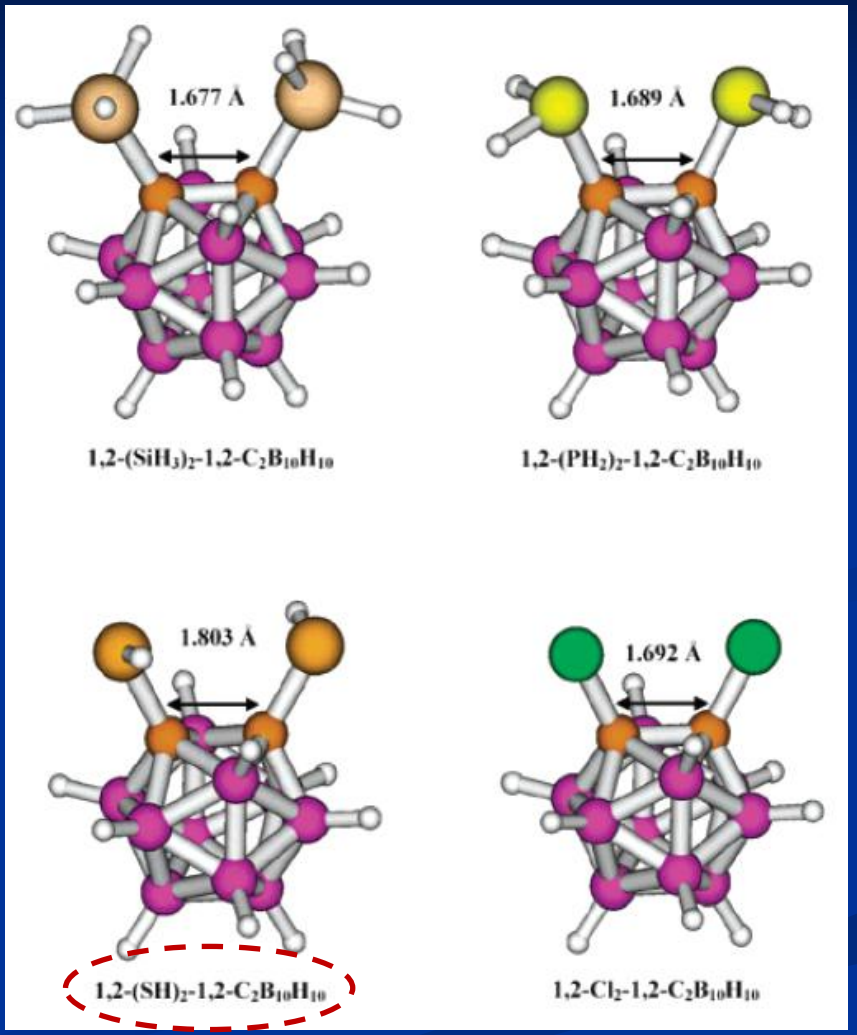

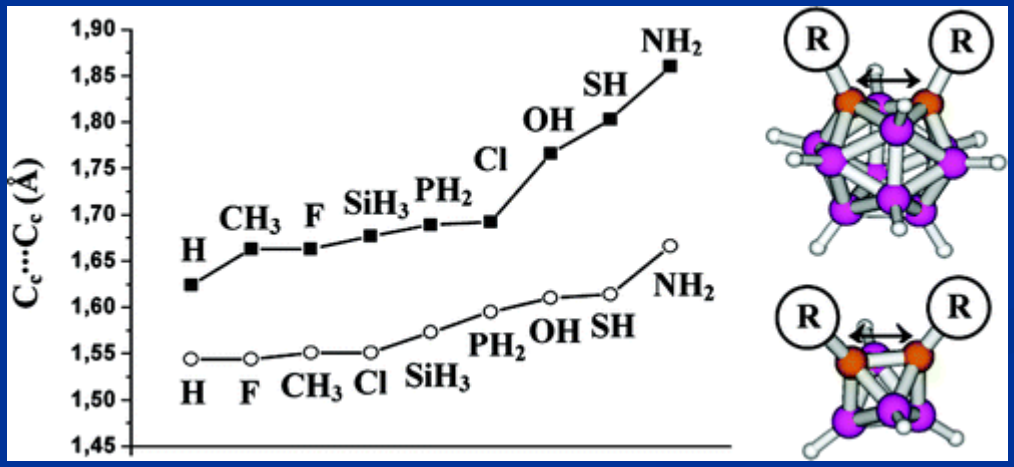

Dianions

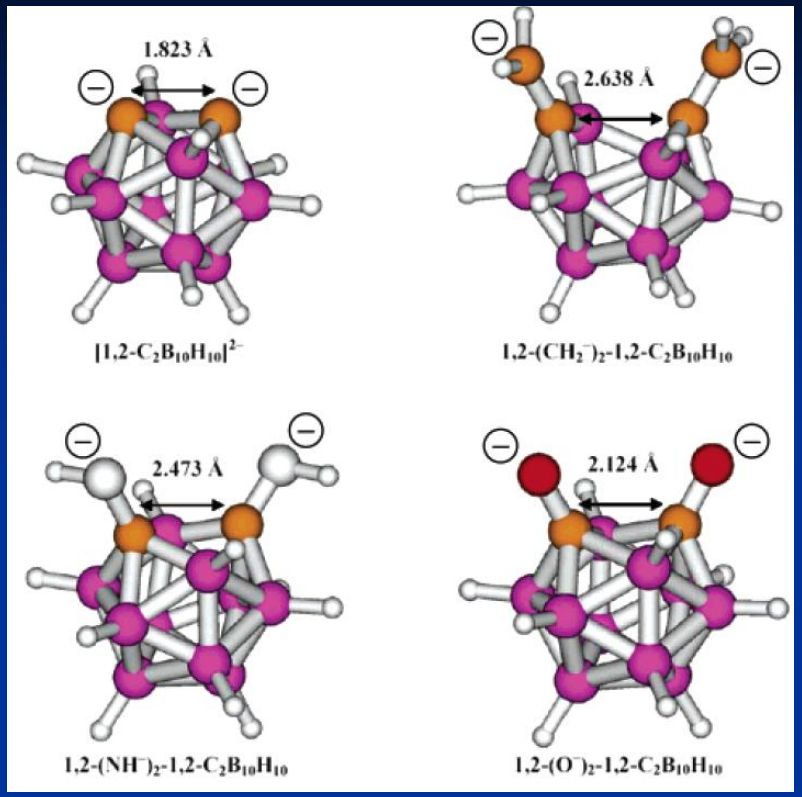
1.823 Å
[1,2-C2B10H10]2−
2.638 Å
1,2-(CH2−)2-1,2-C2B10H10
2.473 Å
1,2-(NH−)2-1,2-C2B10H10
2.124 Å
1,2-(O−)2-1,2-C2B10H10

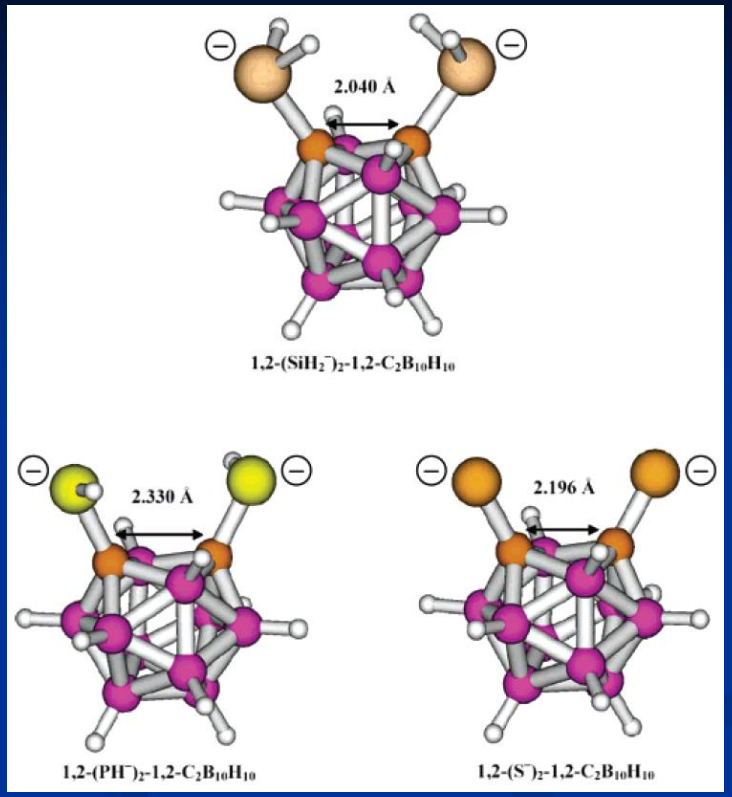
2.040 Å
1,2-(SiH2−)2-1,2-C2B10H10
2.330 Å
1,2-(PH−)2-1,2-C2B10H10
2.196 Å
1,2-(S−)2-1,2-C2B10H10

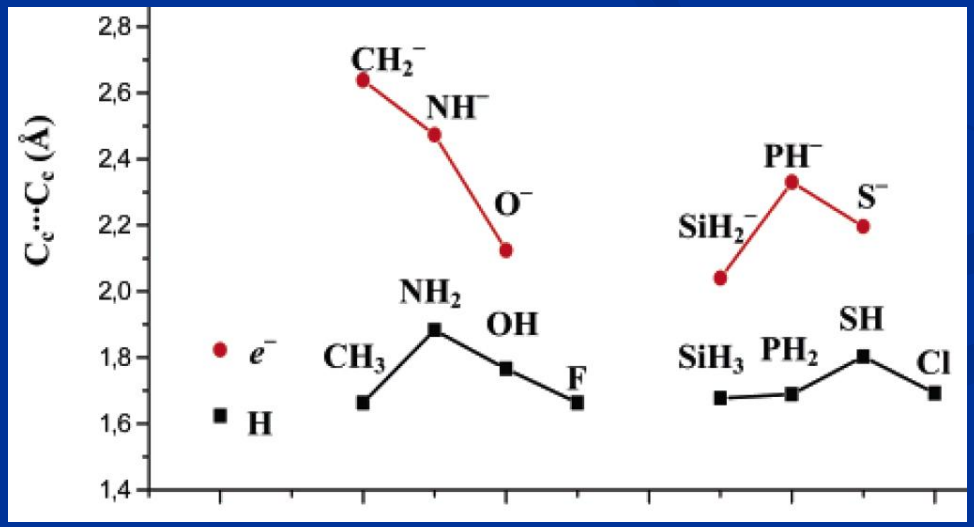
Cc···Cc (Å)
2,8
2,6
2,4
2,2
2,0
1,8
1,6
1,4
CH2−
NH−
O−
PH−
SiH2−
S−
NH2
OH
CH3
F
SH
SiH3
PH2
Cl
e−
H

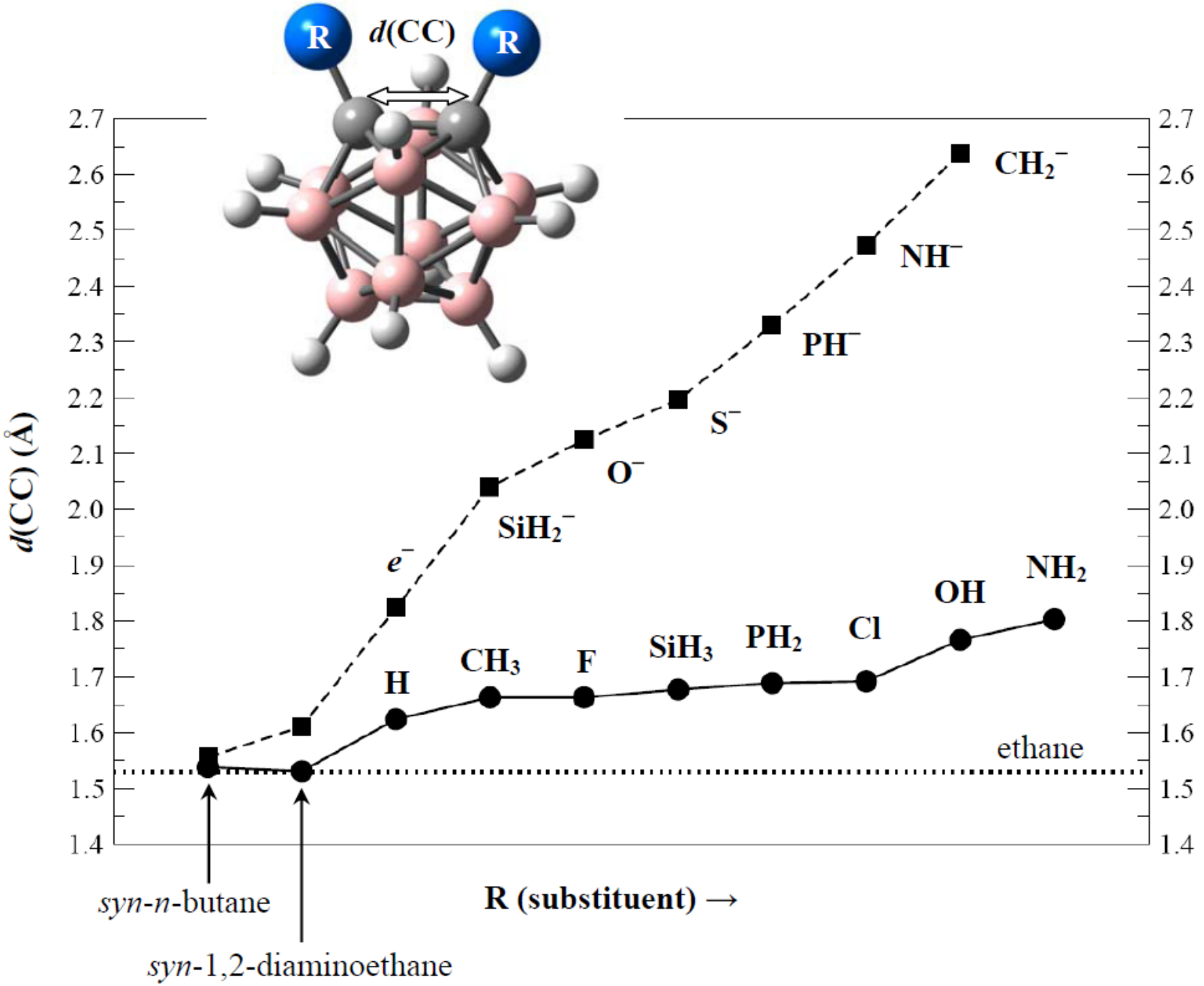
R
d(CC)
R
2.7
2.6
2.5
2.4
2.3
2.2
2.1
2.0
1.9
1.8
1.7
1.6
1.5
1.4
d(CC) (Å)
CH2−
NH−
PH−
S−
O−
SiH2−
e−
NH2
OH
Cl
PH2
SiH3
F
CH3
H
ethane
syn-n-butane
syn-1,2-diaminoethane
R (substituent) →

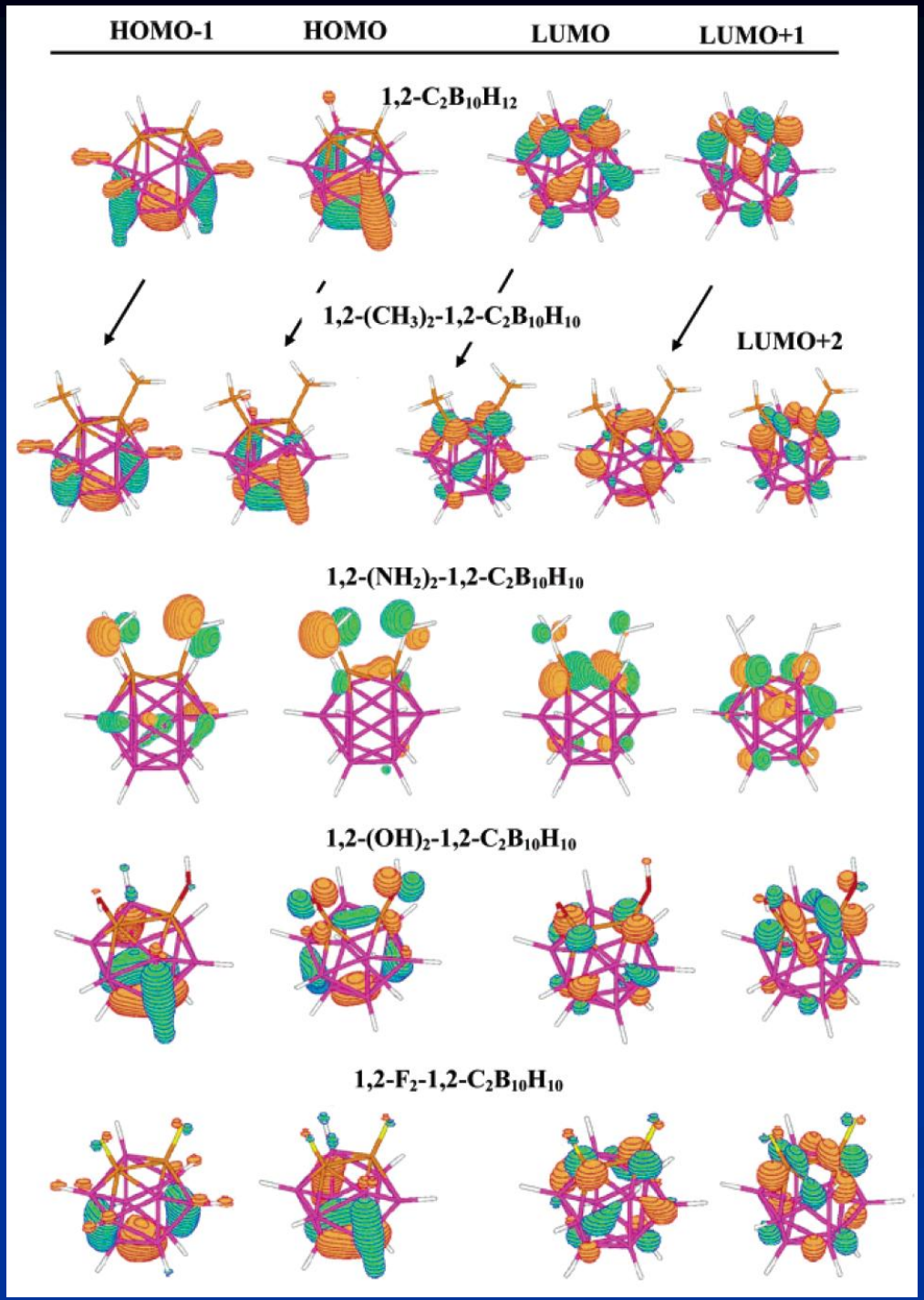

MO analysis

Topological Analysis

- ★ Ring Critical Point
- • Bond Critical Point

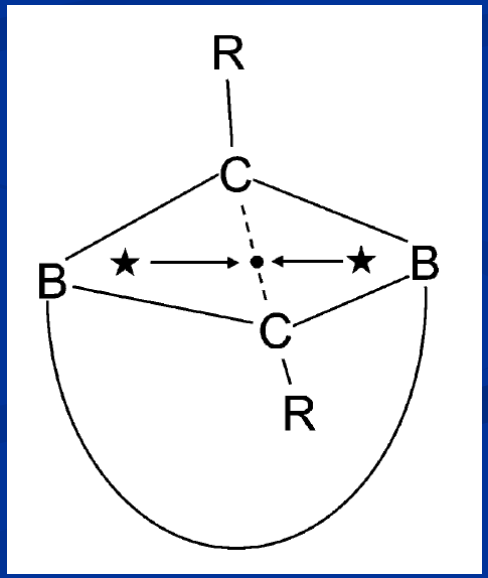

Biradicals derived from Monomers and Dimers of *r* - $C_2B_{10}H_{12}$, *r* = {*ortho*, *meta*, *para*}

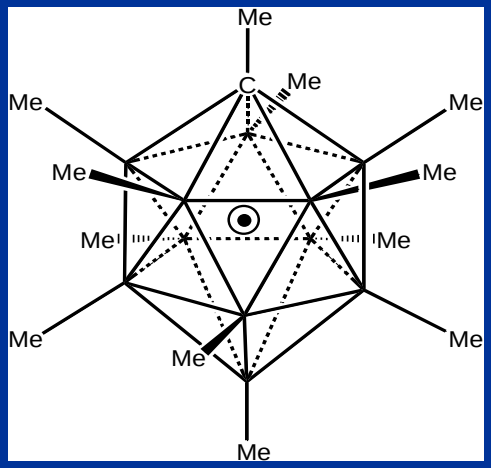

X 2

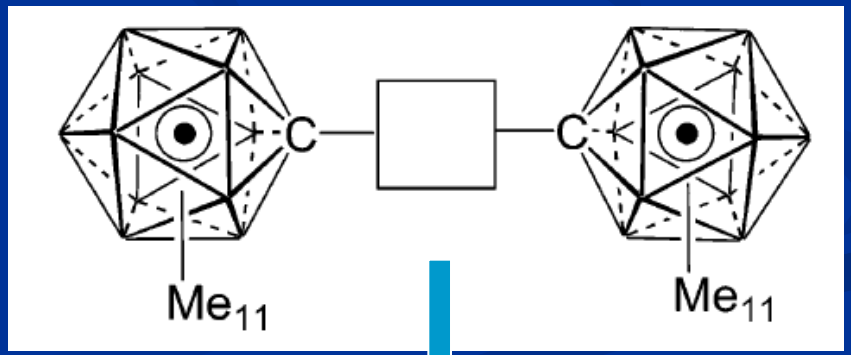

□ = { -C≡C-, -CH=CH- }

"Broken-Symmetry" – "Spin-Projected" Method

$$\Psi_{\mathrm{unr,S}} = a\Psi_{\mathrm{S}} + b\Psi_{\mathrm{T}} \qquad \text{with} \qquad a^2 + b^2 = 1$$

$$b^2 = \frac{1}{2}\langle \Psi_{\mathrm{unr,S}} | \hat{S}^2 | \Psi_{\mathrm{unr,S}} \rangle$$

$$E_{\mathrm{unr,S}} = \langle \Psi_{\mathrm{unr,S}} | \hat{H} | \Psi_{\mathrm{unr,S}} \rangle = a^2 \langle \Psi_{\mathrm{S}} | \hat{H} | \Psi_{\mathrm{S}} \rangle + b^2 \langle \Psi_{\mathrm{T}} | \hat{H} | \Psi_{\mathrm{T}} \rangle$$

$$E_{\mathrm{S}} = \langle \Psi_{\mathrm{S}} | \hat{H} | \Psi_{\mathrm{S}} \rangle = \frac{E_{\mathrm{unr,S}} - b^2 E_{\mathrm{T}}}{1 - b^2}$$

Singlet-Triplet Energy Gap

$$\Delta_{\mathrm{ST}} = E_{\mathrm{S}} - E_{\mathrm{T}} = \frac{E_{\mathrm{unr,S}} - E_{\mathrm{T}}}{1 - b^2}$$

Calibration for Singlet Diradicals: CASPT2 ⇔ "Broken-Symmetry" Model

Quantum-Chemical Computations of Singlet-Triplet Energy Gaps

Type I

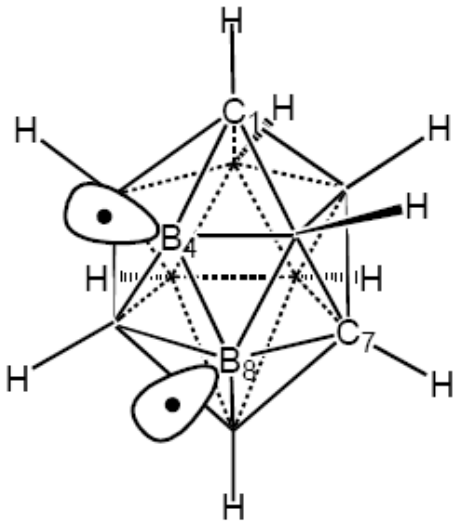

$\Delta E_{ST} = 0.37\ eV$

Type II

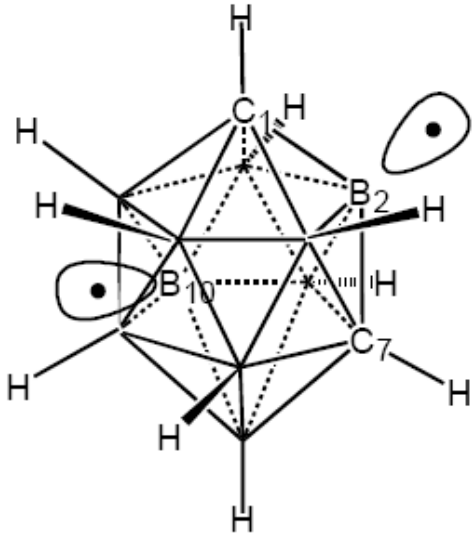

$\Delta E_{ST} = 0.04\ eV$

Type III

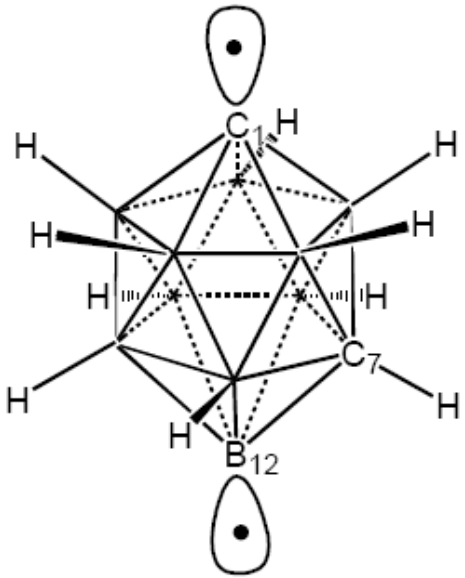

$\Delta E_{ST} = 0.76\ eV$

Broken-Symmetry Solutions Calibrated with CASPT2 computations

Singlet States lower than Triplet States for any Double Hydrogen Removal

Type I

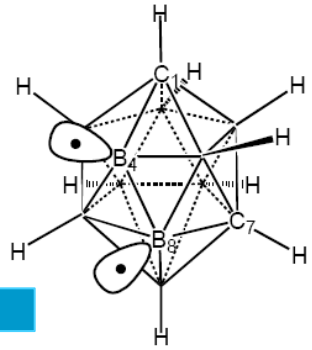

ΔE_{ST} = 0.37 *eV*

Type II

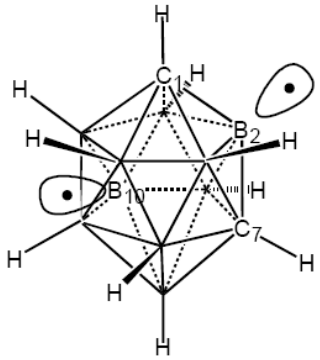

ΔE_{ST} = 0.04 *eV*

Type III

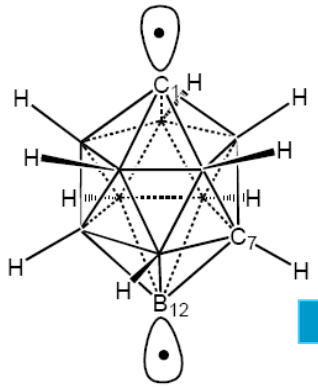

ΔE_{ST} = 0.76 *eV*

HOMO(1.53)

HOMO(1.00)

LUMO(0.47)

LUMO(1.00)

S_0 T_1

m-(4,8) Class Ic

ΔE_{ST} = 0.37 eV

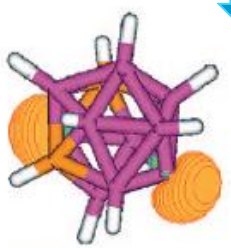

HOMO(1.10)

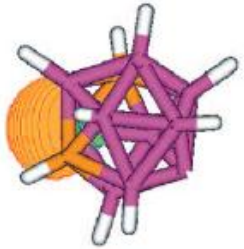

HOMO(1.00)

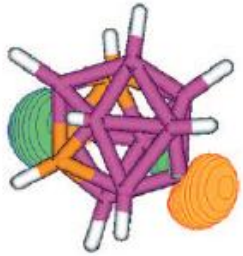

LUMO(0.90)

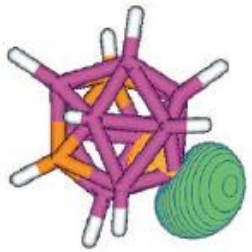

LUMO(1.00)

S_0 T_1

m-(2,10) Class IIc

ΔE_{ST} = 0.04 eV

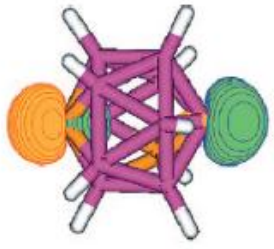

HOMO(1.60)

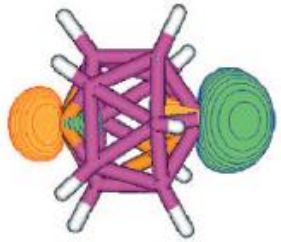

HOMO(1.00)

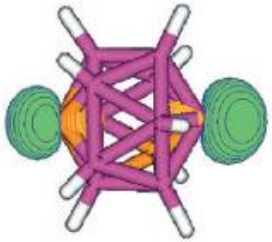

LUMO(0.40)

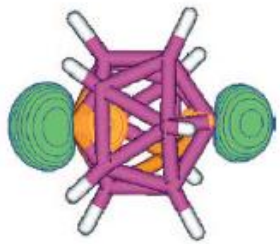

LUMO(1.00)

S_0 T_1

m-(1,12) Class IIIb

ΔE_{ST} = 0.76 eV

Dimers: Unit structure $CB_{11}H_{12}$ → Non-Metal Free (Poly)Radicals

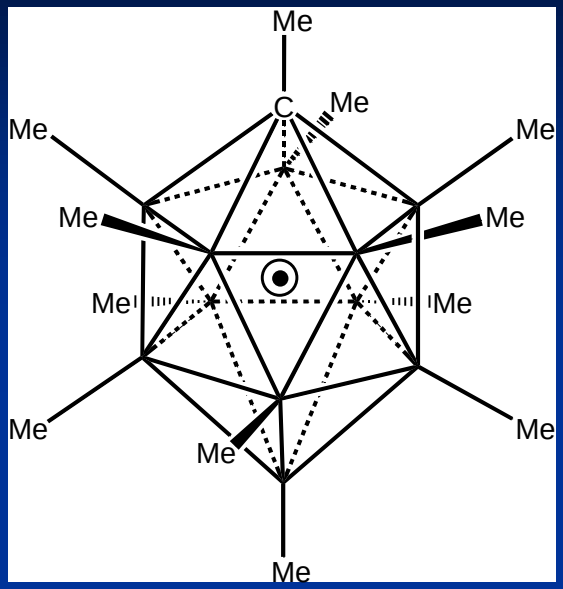

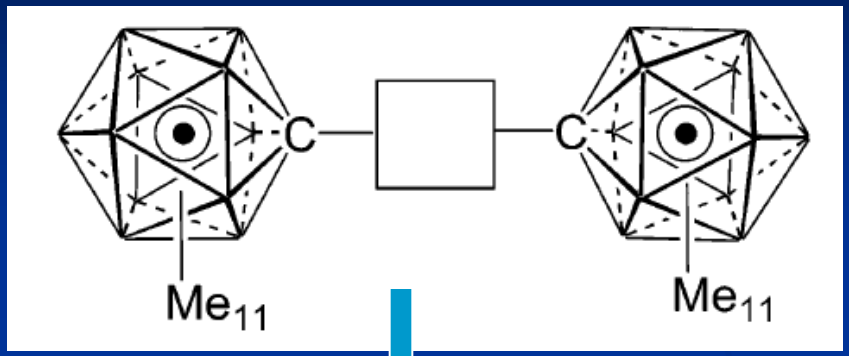

□ = { -C≡C-, -CH=CH- }

ESR Experiments

$$\nu_R = \frac{\Delta E}{h} = \frac{g\mu_B B}{h} = \frac{2.0037 \times (9.3 \times 10^{-24}\,\mathrm{J/T}) \times 37\mathrm{G} \times 10^{-4}\,\mathrm{T/G}}{6.6 \times 10^{-34}\,\mathrm{J \cdot s}} \approx 1.043 \times 10^{8}\,\mathrm{Hz}$$

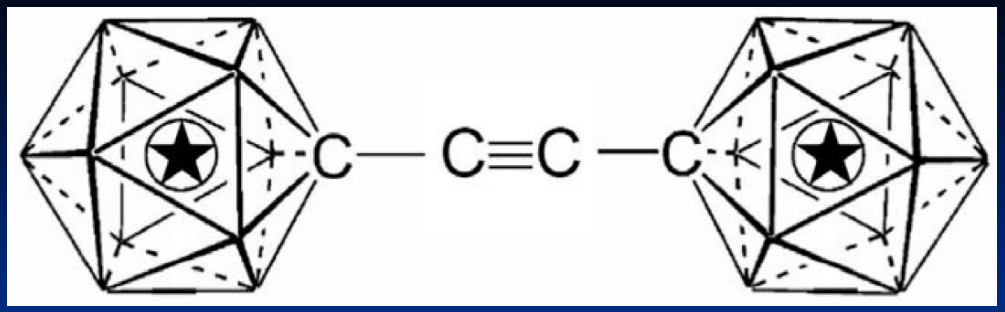

Every vertex → BH

✪ = { ⊙ , – }

Energy as Function of q and S → E = E(q, S)

Table 1
Relative energies (ΔE_r), vertical (ΔE_v) or adiabatic (ΔE_a) singlet–triplet energy gaps (all in eV), and other properties for the low-lying states of the dimers studied in this work at different levels of theory: DFT/(U)B3LYP/6-31+G(d) → DFT and CASPT2//DFT/6-31+G(d) → CP2.

System (q)[a]	$\langle\hat{S}^2\rangle$	PGS[b]	IMAG[b]	$\Delta E_r^{DFT,c}$	$\Delta E_v^{DFT,d}$	ΔE_a^{DFT}	$\Delta E_r^{CP2,c}$	$\Delta E_v^{CP2,d}$	ΔE_a^{CP2}
Dianion									
S_0 (−2)[e]	0.0000	C_2	20i	0.00	5.12	–	0.00	5.51	–
cis-T_1 (−2)	2.0043	C_2	–	–	–	3.79	–	–	3.64
trans-T_1 (−2)	2.0066	C_2	–	–	–	3.78	–	–	3.49
Radical anion									
D_0 (−1)	0.7521	C_2	–	2.83	–	–	3.11	–	–
Neutral biradical									
S_0 (0)[f]	1.0080	C_2	13i	9.19	0.013	–	8.88	0.007	–
T_1 (0)	2.0075	C_s	8i	–	–	**0.004**	–	–	0.005

A closed-shell S_0 (C_{2v}) structure is found with $\langle\hat{S}^2\rangle$ zero 0.04 eV higher in energy than the biradical broken-symmetry solution.

[a] System(q) → singlet (S), doublet (D) or triplet (T) state with charge q.

[b] Point-group symmetry (PGS) and residual imaginary frequency (IMAG) of the optimized structure.

[c] ΔE_r is the relative energy of each compound from the singlet (ground) state of the dianion as the most stable case.

[d] ΔE_v is the singlet–triplet gap at the singlet (ground) state geometry.

[e] For the singlet dianion the pure DFT/(U)B3LYP and broken-symmetry solutions are equivalent.

[f] Broken-symmetry solution. The DFT singlet–triplet energy gaps are approximated as $\Delta E = 2(E_{BS} - E_T)/(\langle\hat{S}^2\rangle_T - \langle\hat{S}^2\rangle_{BS})$.

$-\Delta E_{ST} \sim 0.005$ eV < $k_B T$ (0.025 eV)

Neutral Biradical with -HC=CH- bridge

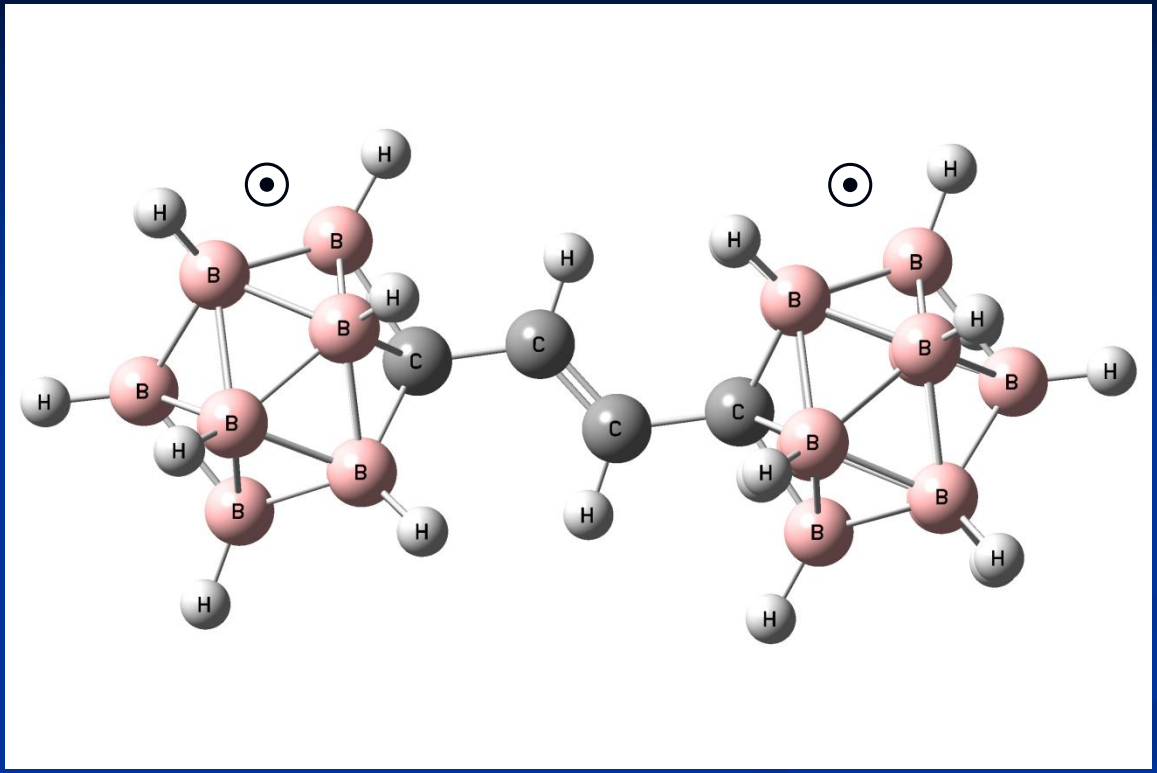

E_T = -713.817812 au

$E_{unr,S}$ = -713.819606 au

$\langle \hat{S}^2 \rangle_{unr,S}$ = 0.7818

UB3LYP/6-31+G(d) Computations

$$\Delta_{ST} = E_S - E_T = \frac{E_{unr,S} - E_T}{1 - b^2} = \textbf{-0.003 eV}$$

$$\Delta_{DQ} = E_{1/2} - E_{3/2} = \frac{E_{unr,S=1/2} - E_{3/2}}{1 - b^2} = \frac{12 \cdot (E_{unr,S=1/2} - E_{3/2})}{15 - 4 \cdot \left\langle \hat{S}^2 \right\rangle_{unr,S=1/2}}.$$

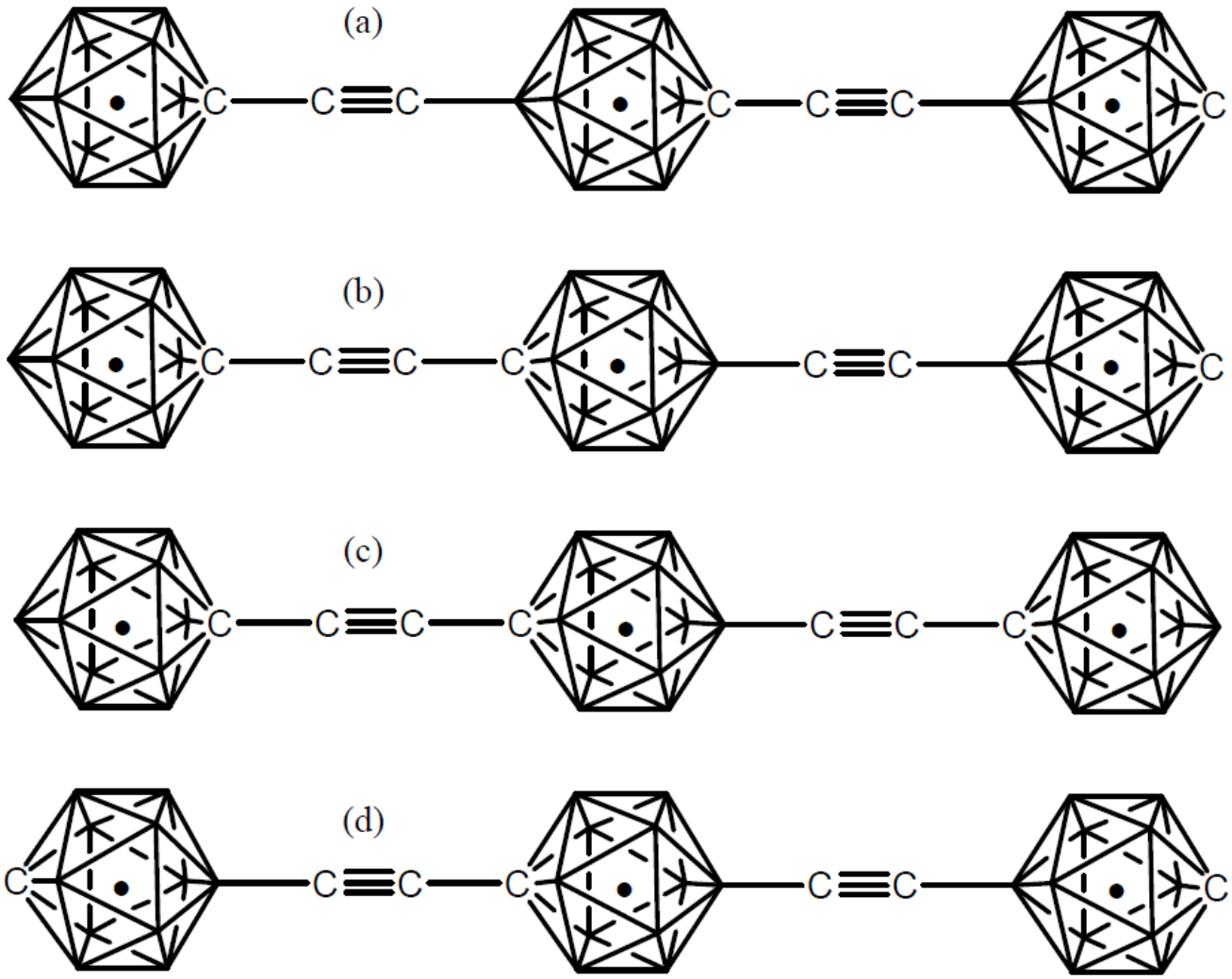

Figure 6. The four trimers derived from the two posible orientations A/B of carborane $CB_{11}H_{12}^{\bullet}$ (s=1/2) – see Figure 5 above – connected through acetylene bridge unions: (a) A-CC-A-CC-A, (b) A-CC-B-CC-A, (c) A-CC-B-CC-B, and (d) B-CC-B-CC-A. The dot in each cage representes one unpaired electron.

ΔE_{DQ} (eV)

+0.02

–0.015

–0.011

–0.054

far-IR

Cyclic Polyradical Systems

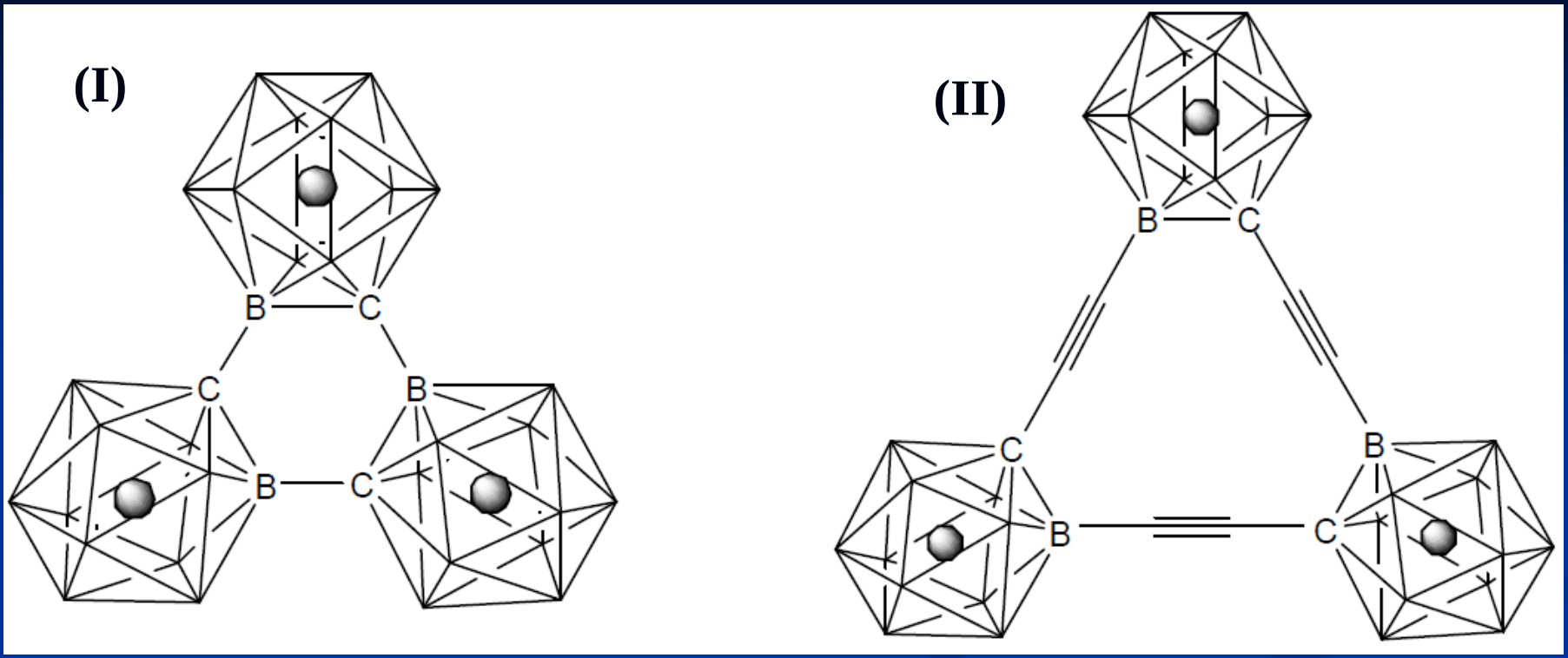

System, Spin	Energy (au)	$\langle \hat{S}^2 \rangle$	ΔE (eV)
(I)	-952.829852	3.76	---
(I)	-952.829762	1.76	0.004
System, Spin	**Energy (au)**	$\langle \hat{S}^2 \rangle$	**ΔE (eV)**
(II)	-1181.351576	3.76	0.030
(II)	-1181.350845	1.75	---

UB3LYP/6-31G method*

1D Heteroborane Chains with Transition Metals

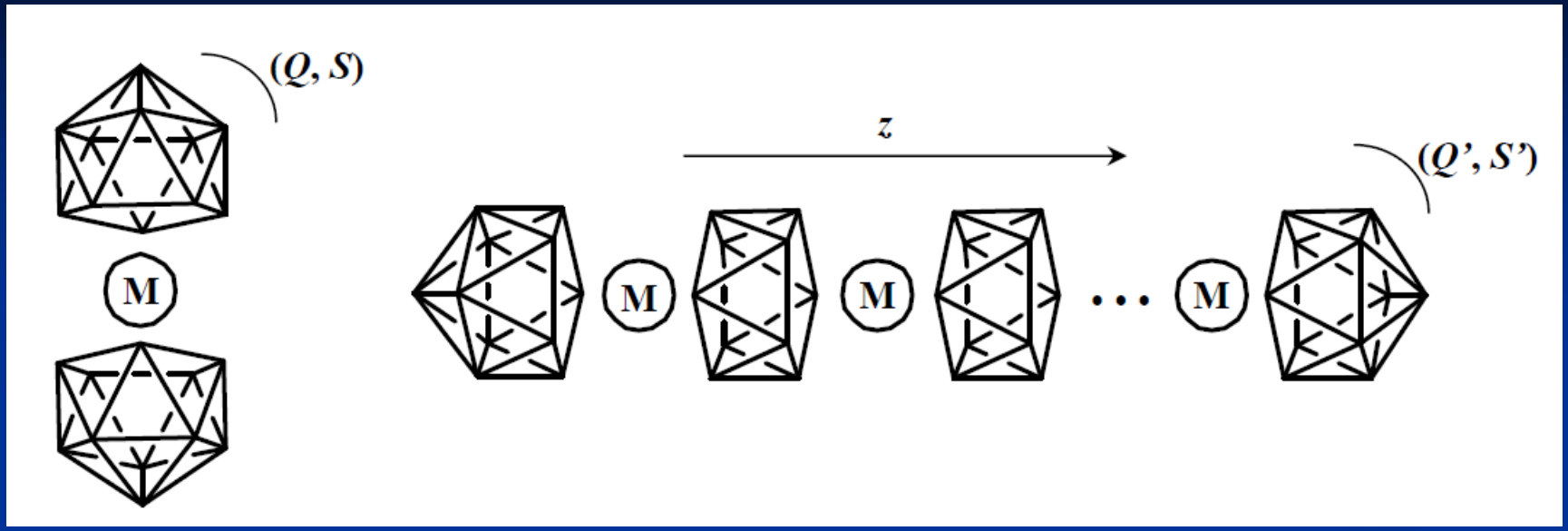

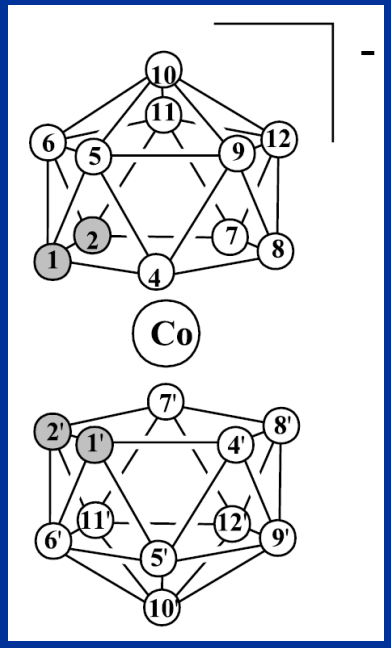

$[commo\text{-}3,3'\text{-}Co(1,2\text{-}C_2B_9H_{11})_2]^-$

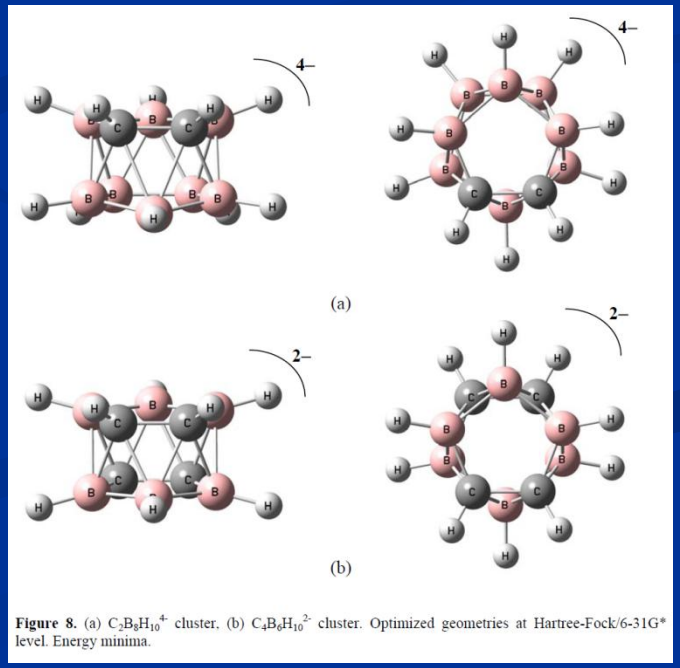

Figure 8. (a) $C_2B_8H_{10}^{4-}$ cluster, (b) $C_4B_6H_{10}^{2-}$ cluster. Optimized geometries at Hartree-Fock/6-31G* level. Energy minima.

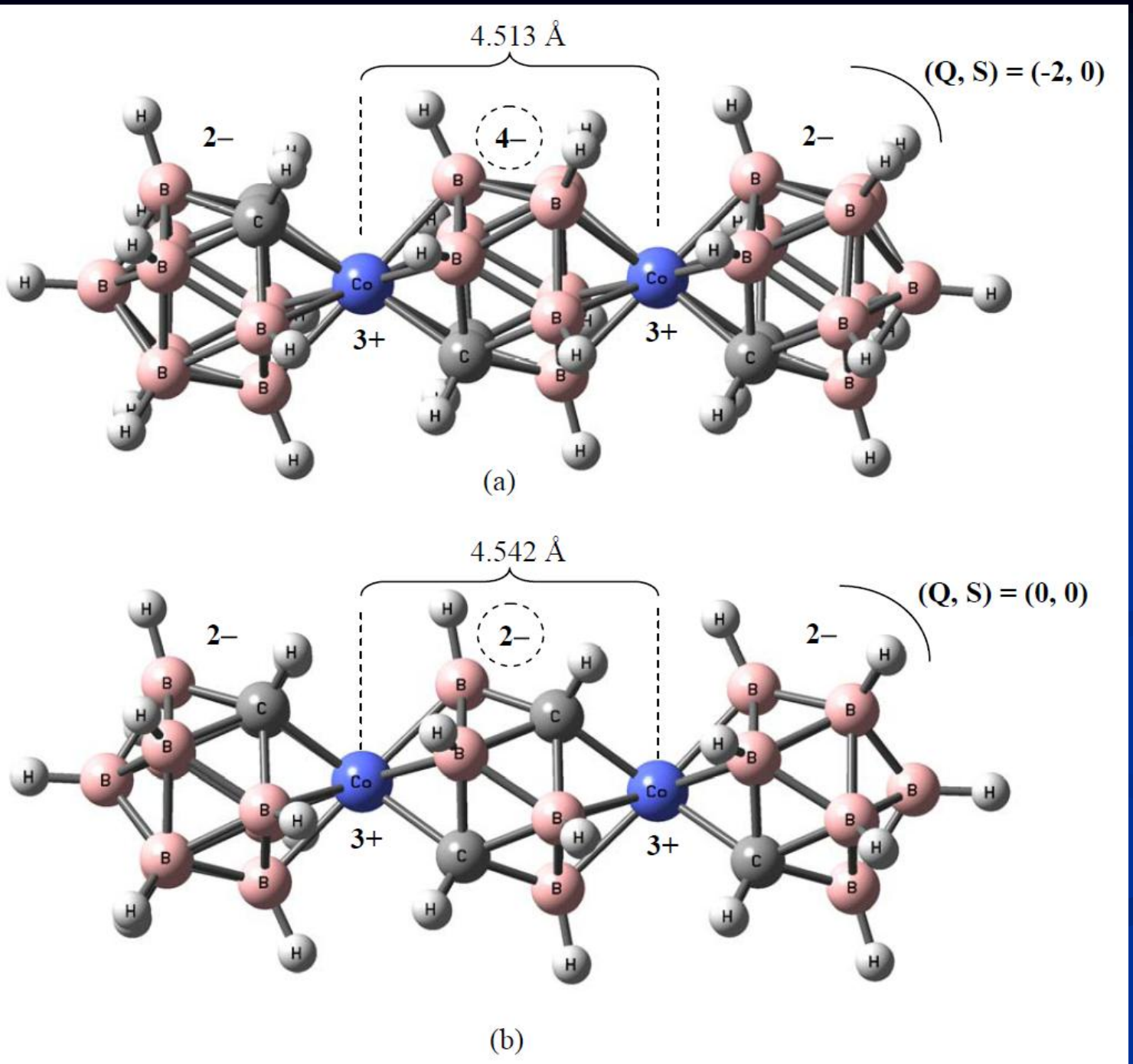
4.513 Å
(Q, S) = (-2, 0)
2–
4–
2–
Co
Co
3+
3+
(a)
4.542 Å
(Q, S) = (0, 0)
2–
2–
2–
Co
Co
3+
3+
(b)

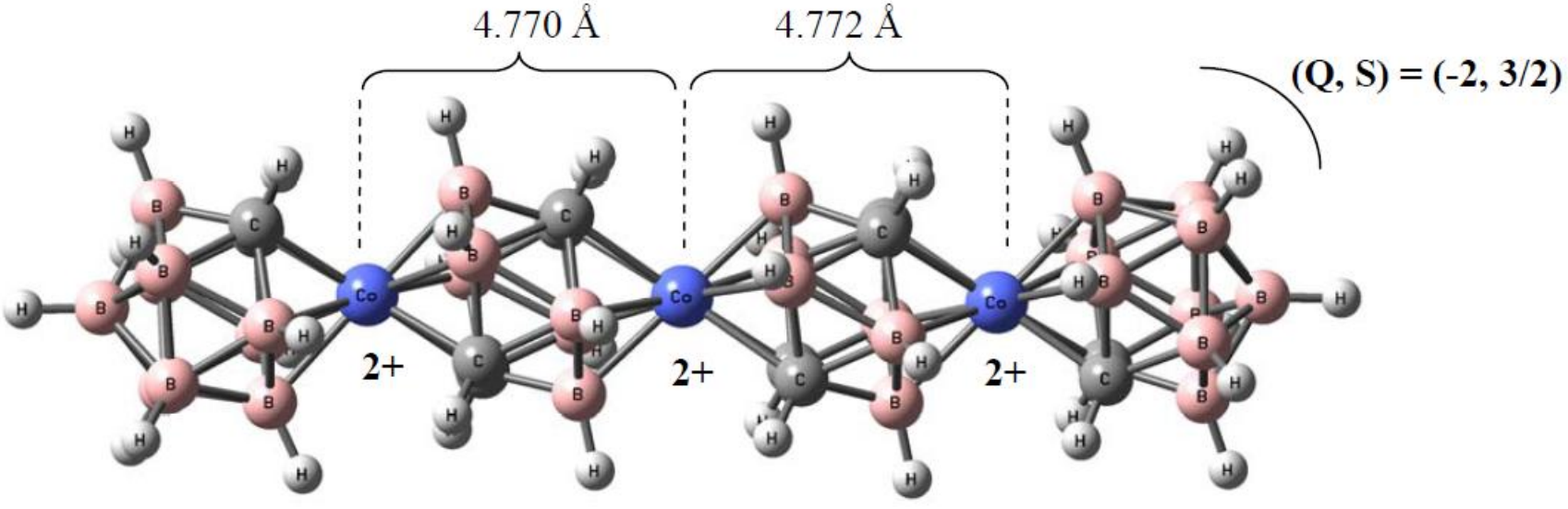

(a)

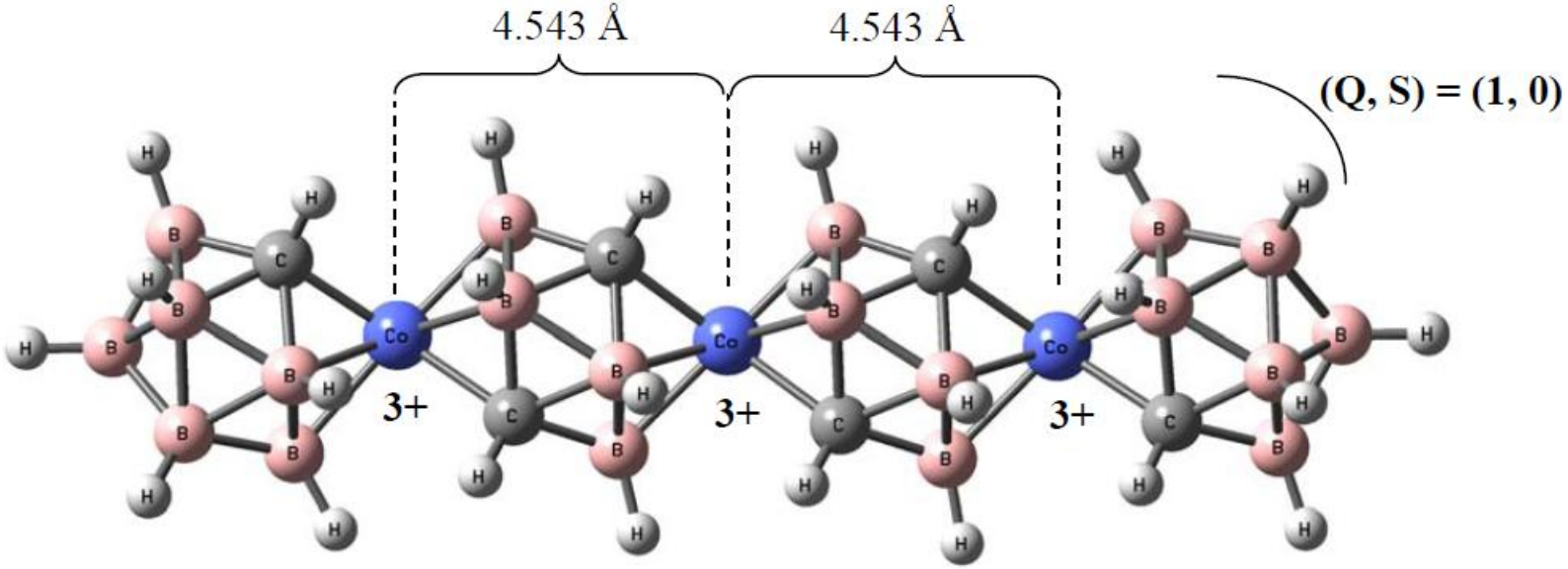

Tetrahedron Supercluster: $[\{(H_9B_{11}C)C{\equiv}C\}^{\odot}]_4$

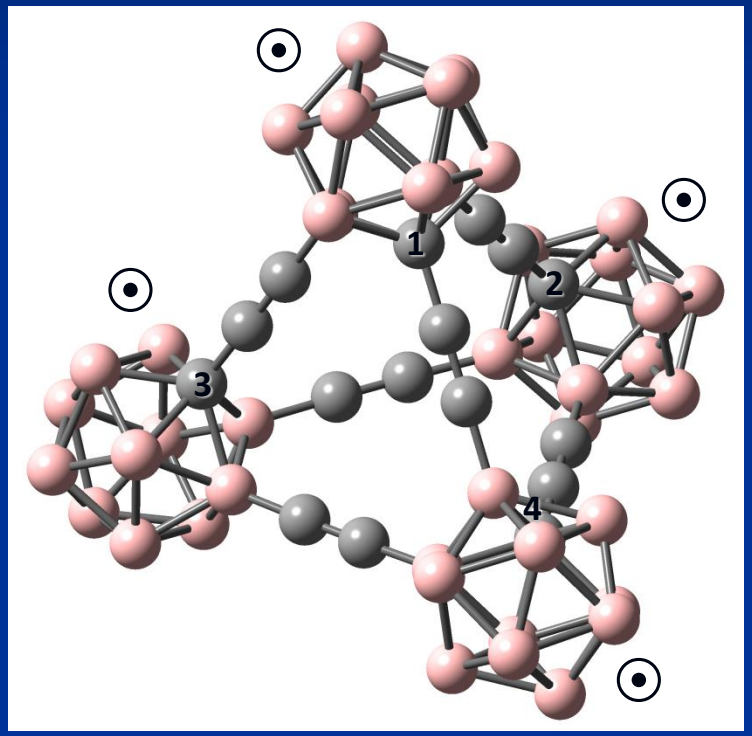

E(q = -4, S = 0) = -1725.452994 au

q = -3, S = ½

q = -2, S = 1

q = -1, S = 3/2

q = 0, S = 2

Map onto model Hamiltonian (Heisenberg – Dirac - Van Vleck):

$$\hat{H}_{spin} = \sum_{i,j} -J_{ij}\hat{S}_i \cdot \hat{S}_j$$

Origin Chemical Bond ⟷ Quantum Effect

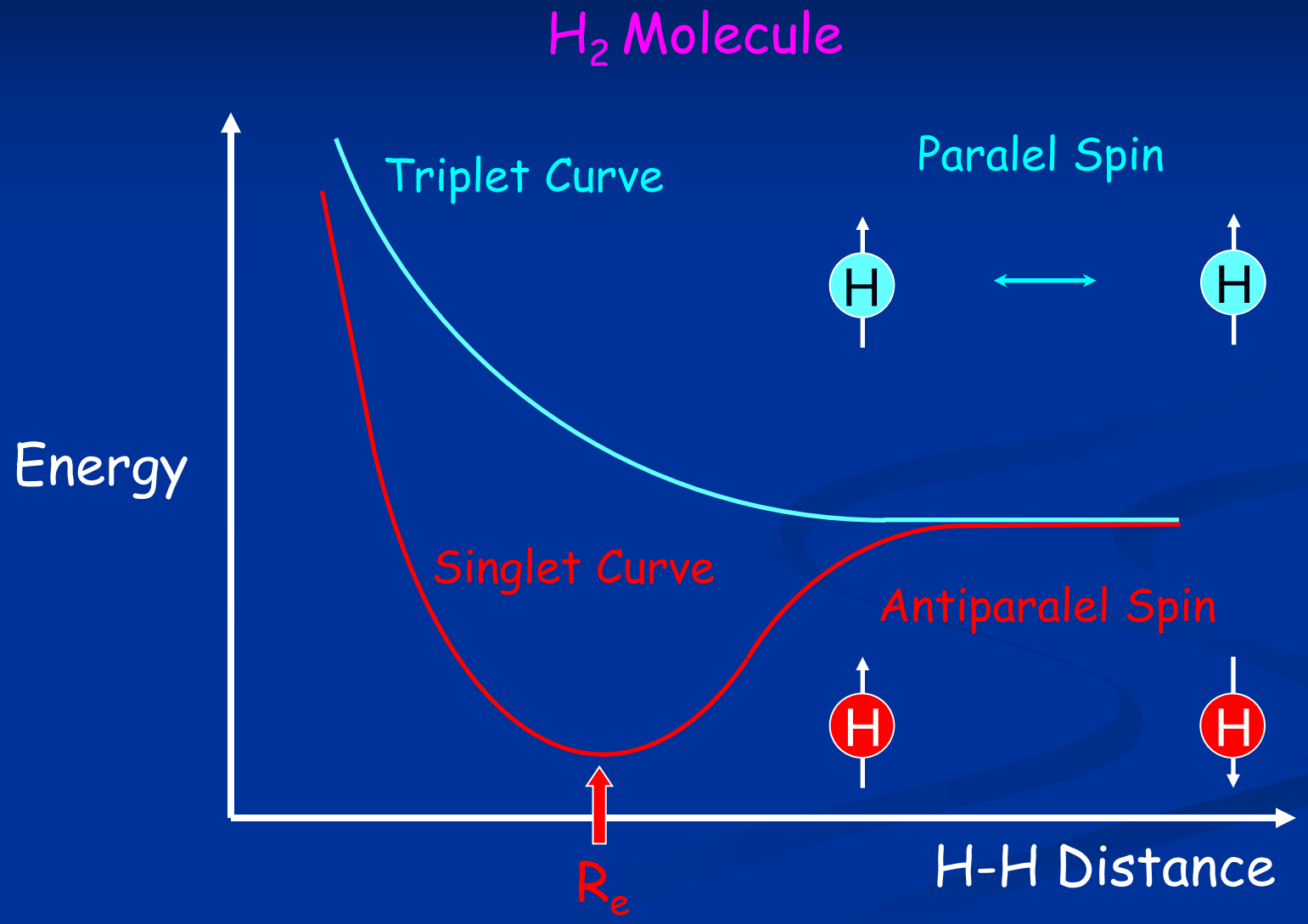

Dissociation: $H_2 \rightarrow H + H$

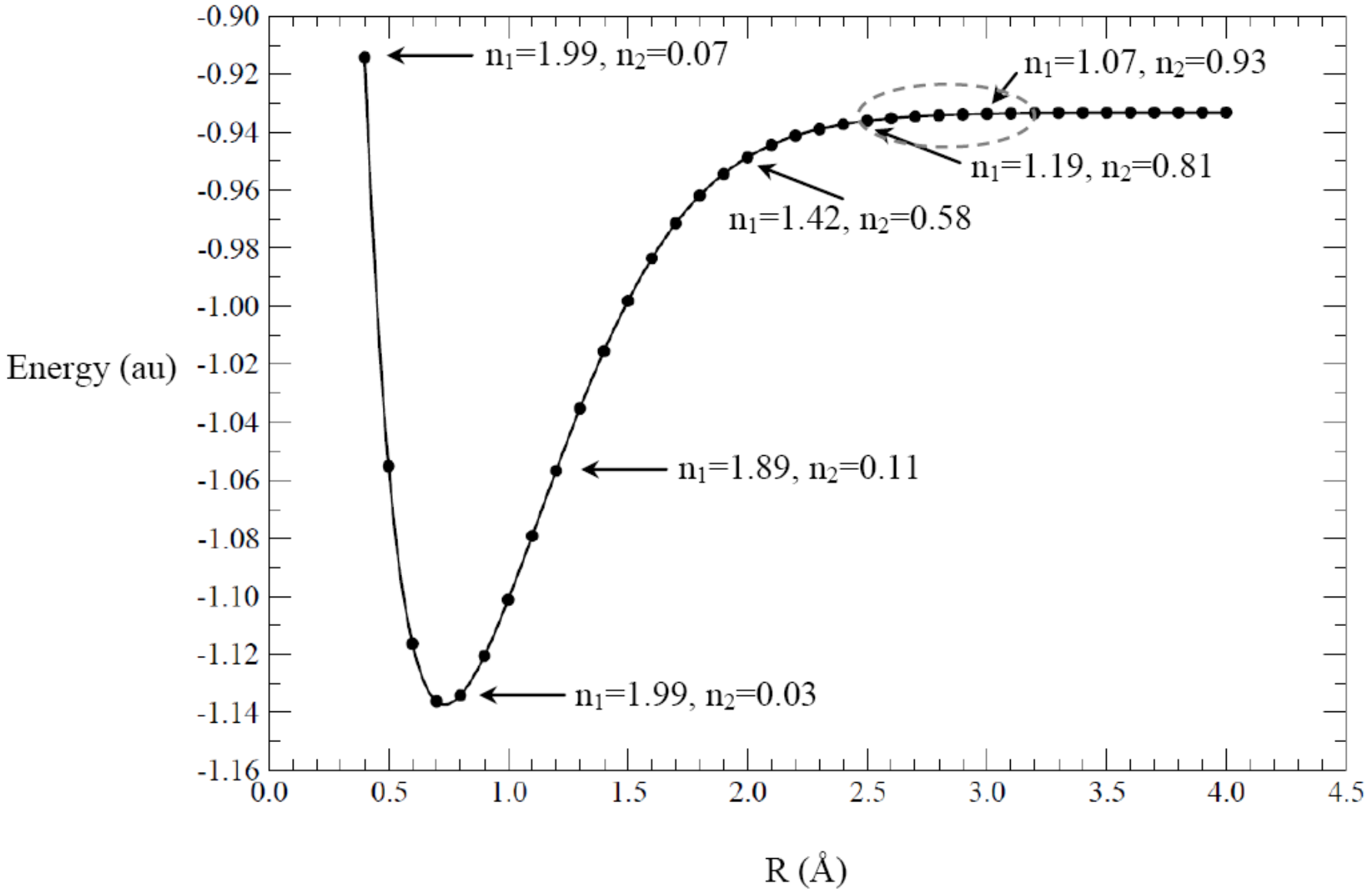

Model System: H_n clusters → Map onto 1D, 2D and 3D Boron Cluster Architectures

Polyhedrons considered here:

i) Planar Cycles : Perfect triangle, square, pentagon and hexagon

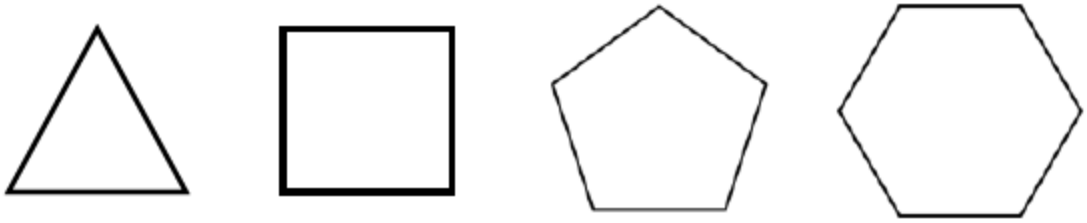

ii) 3D Polyhedra: Octahedron, cube and icosahedron

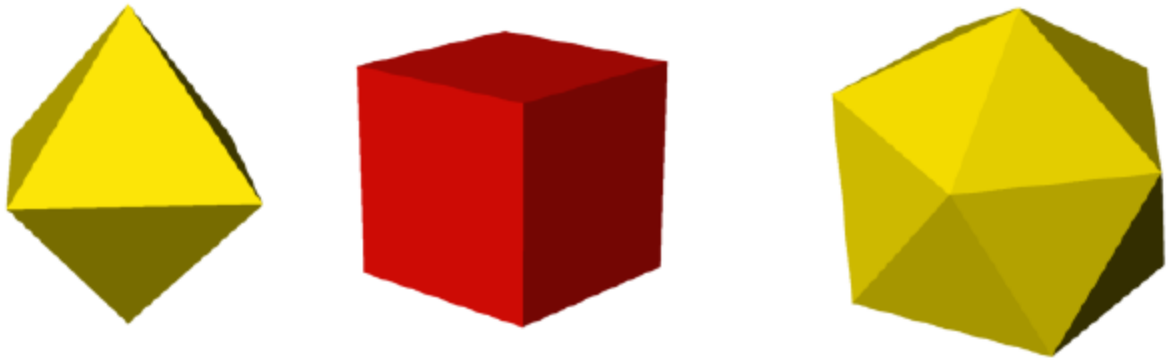

(ii) Endohedral Complexes

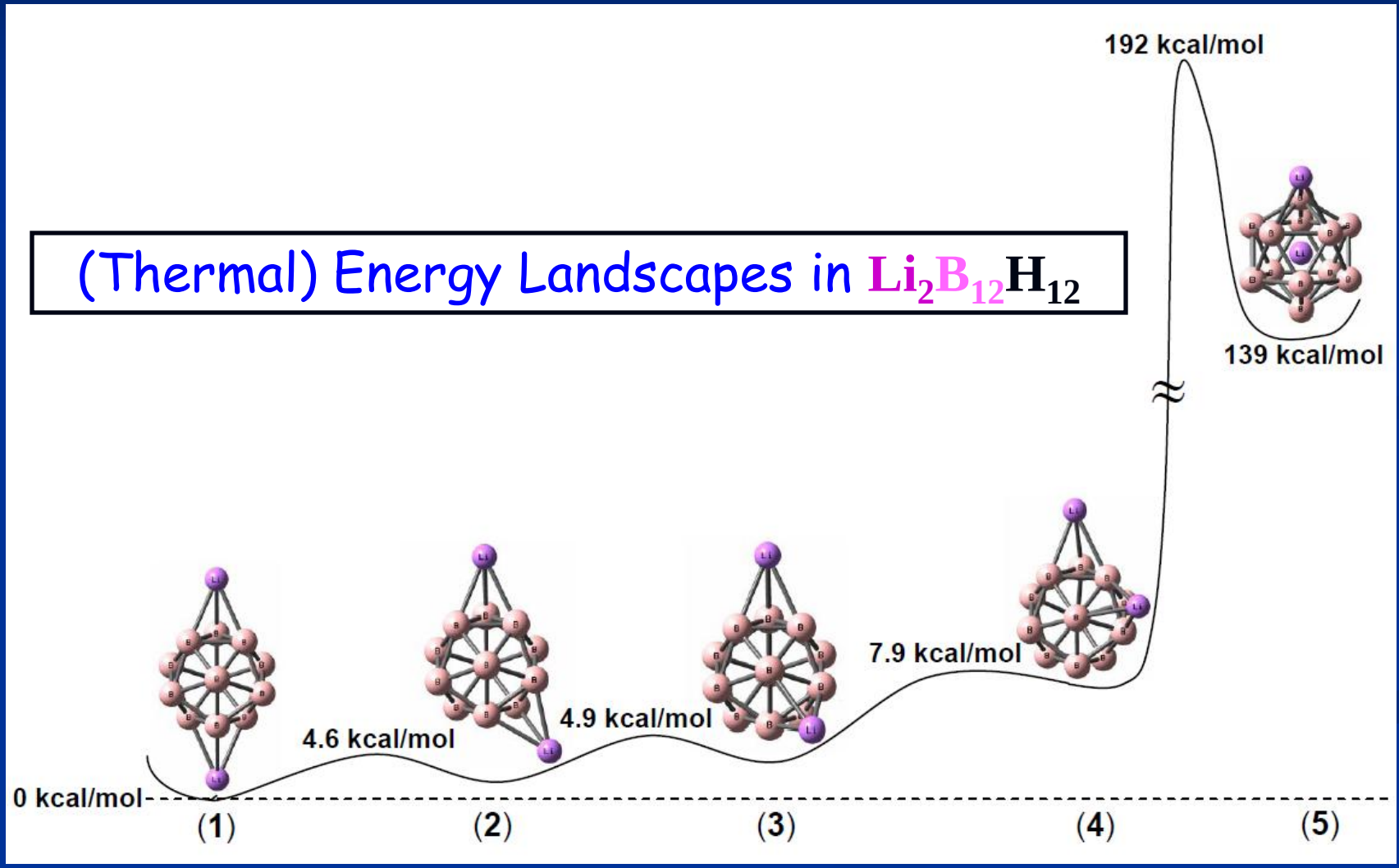

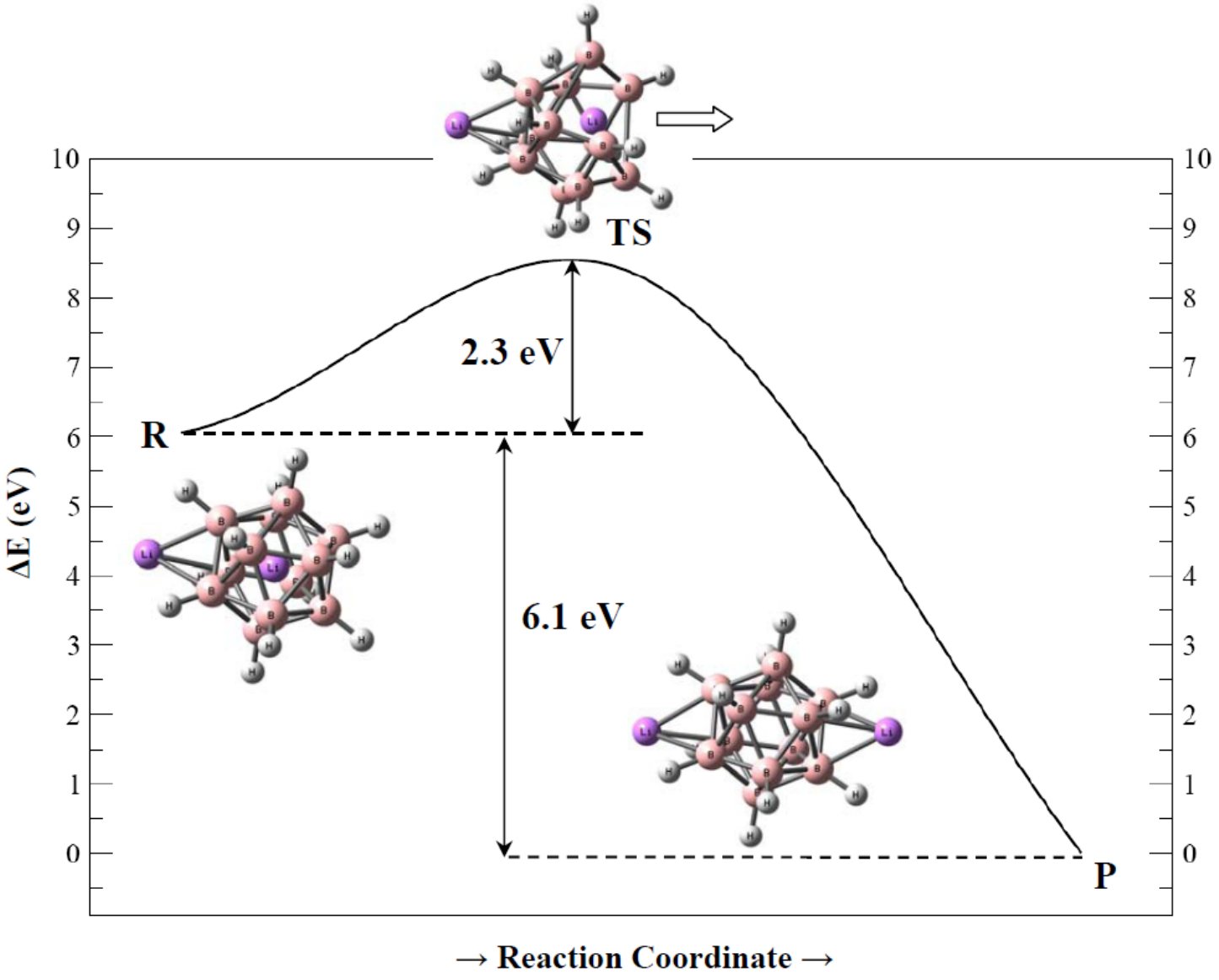

Figure 2. Energy landscape - to scale - in $Li_2B_{12}H_{12}$ groundstate S_0: Thermal ejection mechanism $Li[Li@B_{12}H_{12}] \rightarrow Li_2B_{12}H_{12}$, showing reactant (R, *exo*/*endo* complex), transition state (TS) and product (P, *diexo* complex). B3LYP/6-311+G(d,p) computations.

(Photochemical) Energy Landscapes in $LiCB_{11}H_{12}$

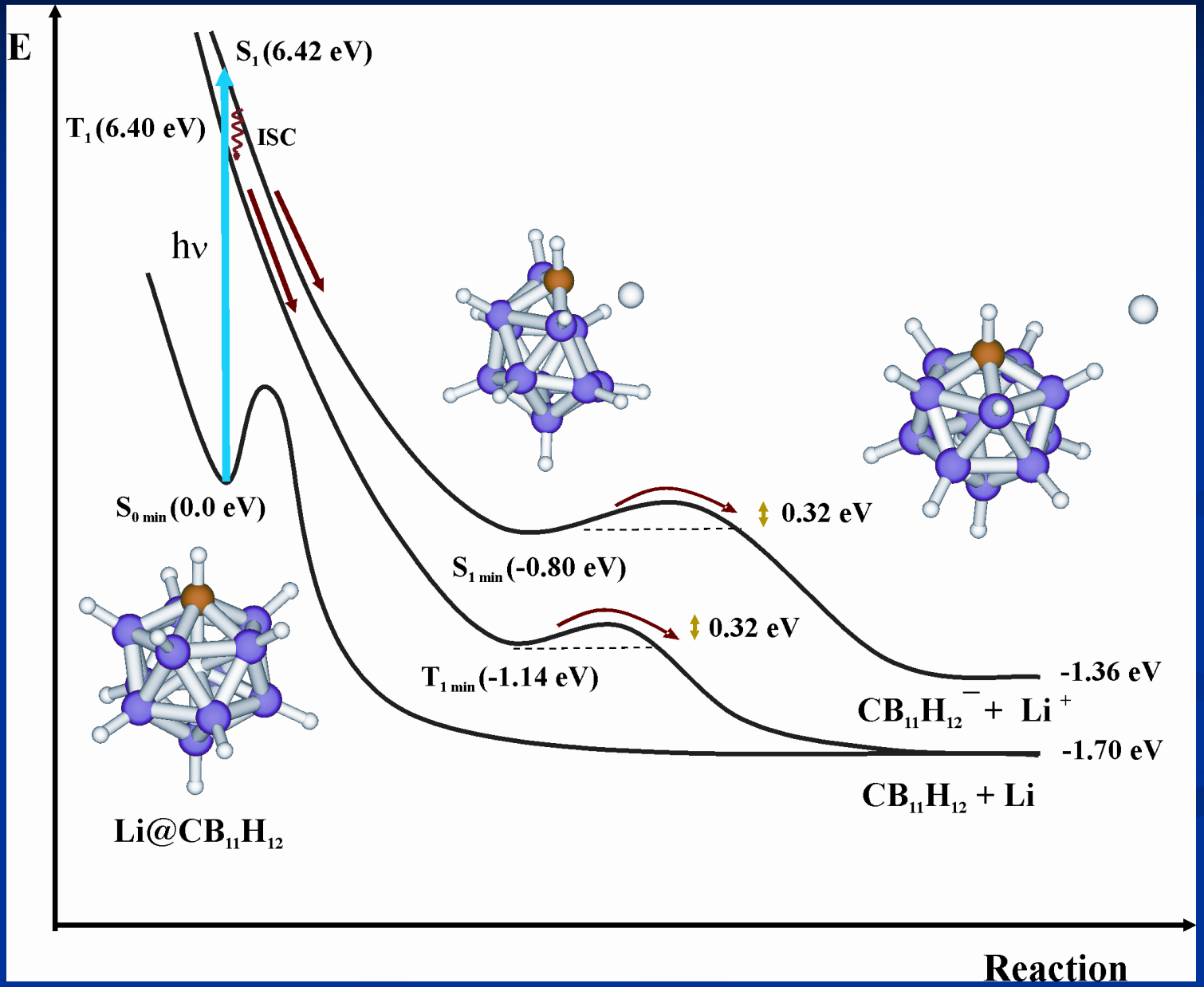

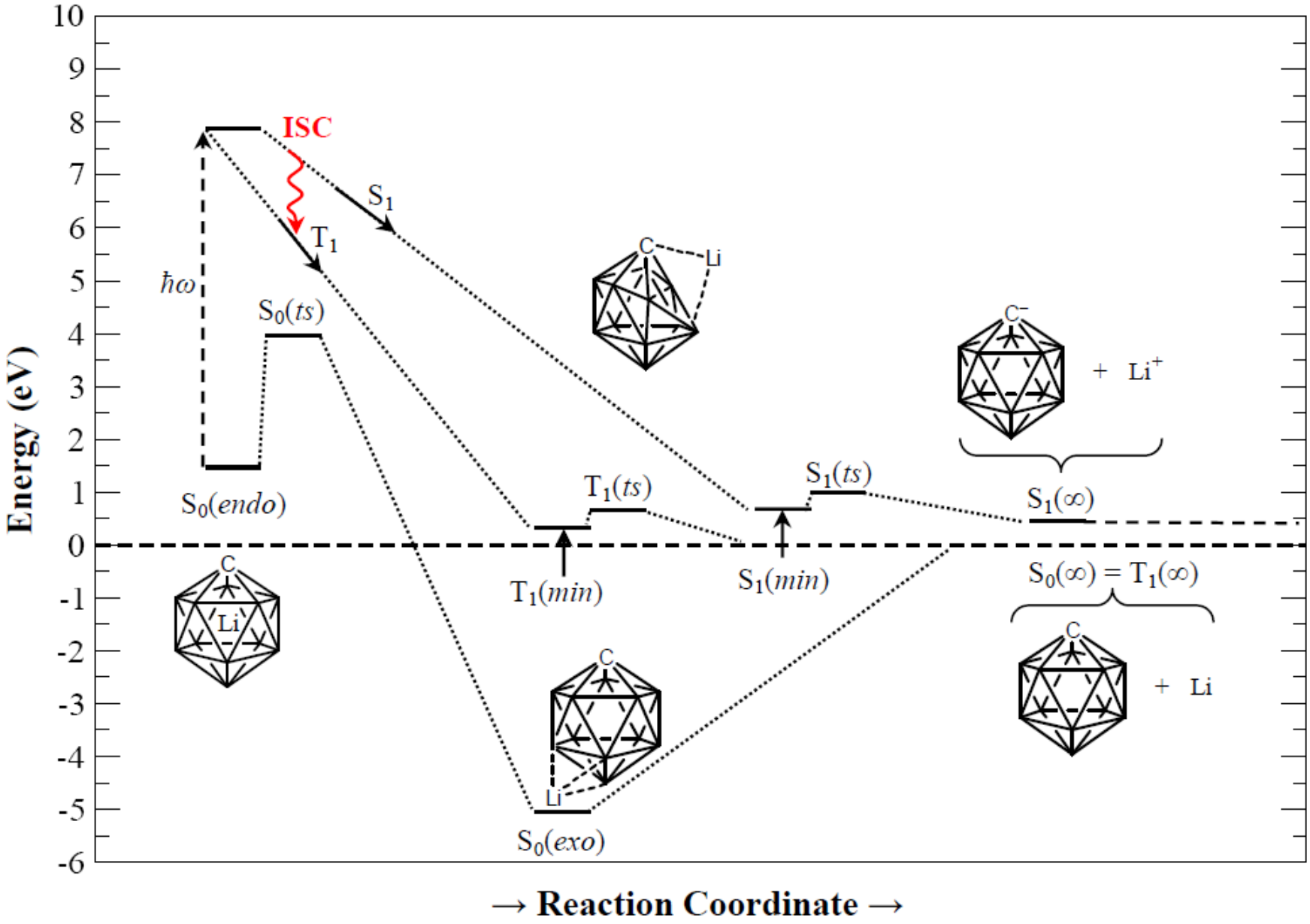
10
9
8
7
6
5
4
3
2
1
0
-1
-2
-3
-4
-5
-6
Energy (eV)
ISC
S1
T1
ħω
S0(ts)
S0(endo)
T1(ts)
T1(min)
S1(ts)
S1(min)
S1(∞)
S0(∞) = T1(∞)
S0(exo)
C
Li
C–
+ Li+
+ Li
→ Reaction Coordinate →

Energy Landscapes from Solid State Chemistry

$[Sc@B_{24}H_{24}]^{+}$

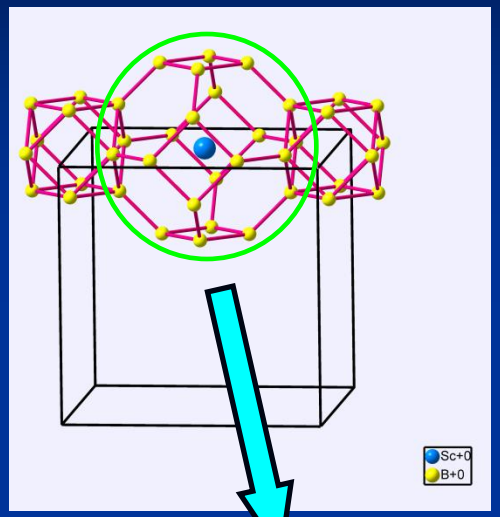

The crystal structure of ScB_{12} consists of fused large B_{24} and small B_{12} truncated octahedra and cubes respectively

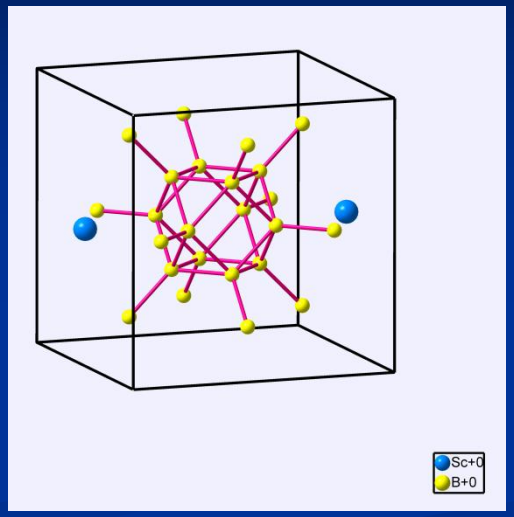

Energy Minima

O sym

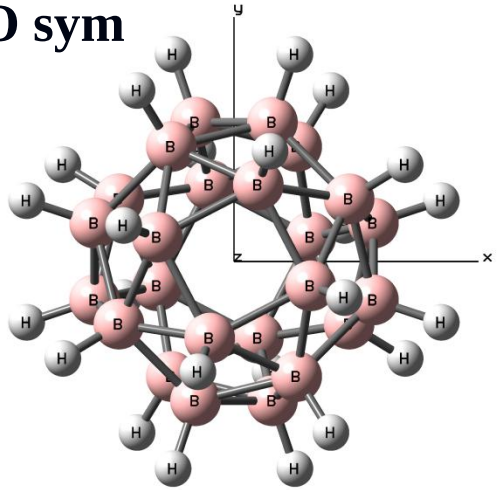

$[B_{24}H_{24}]^{2-}$

Sc^{3+}

$[Sc@B_{24}H_{24}]^{+}$

O sym

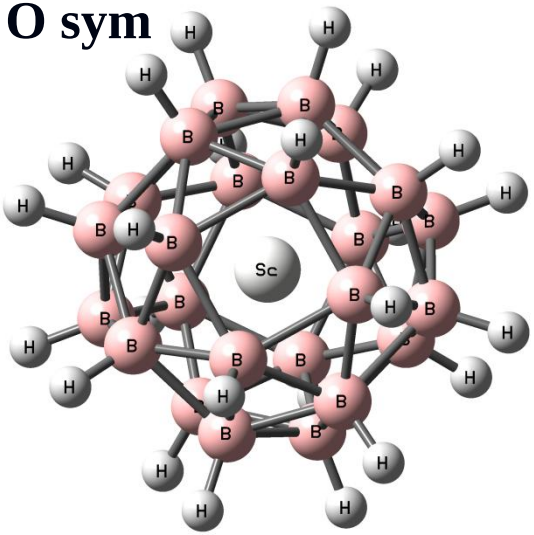

(Excited State) Energy Landscapes of $B_{18}H_{22}$ isomers

anti - $B_{18}H_{22}$

syn - $B_{18}H_{22}$

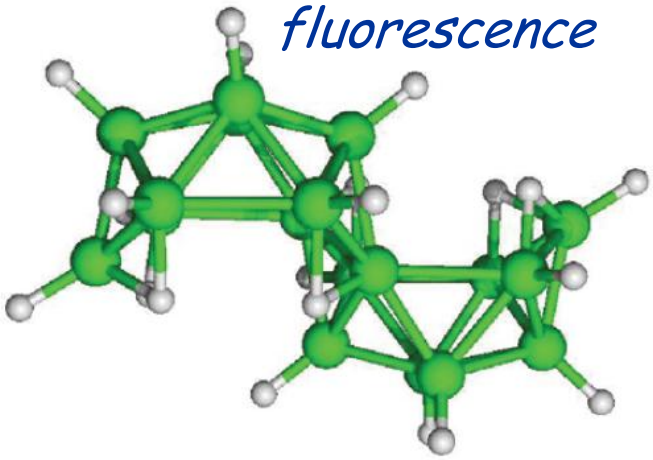

fluorescence

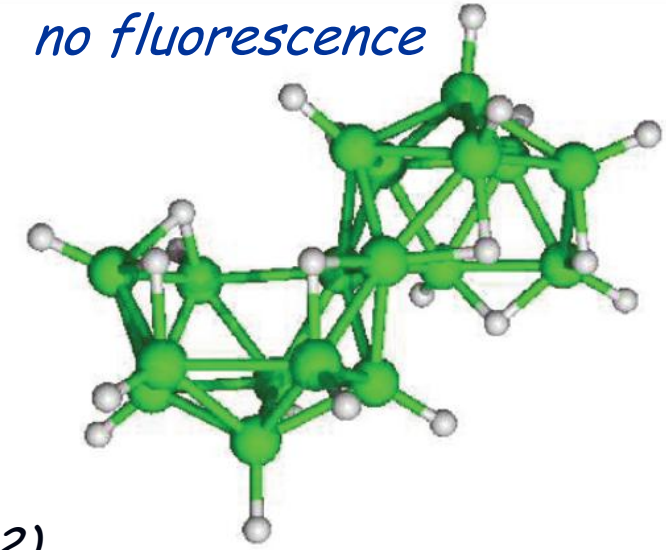

no fluorescence

Pitochelli, Hawthorne, JACS (1962)

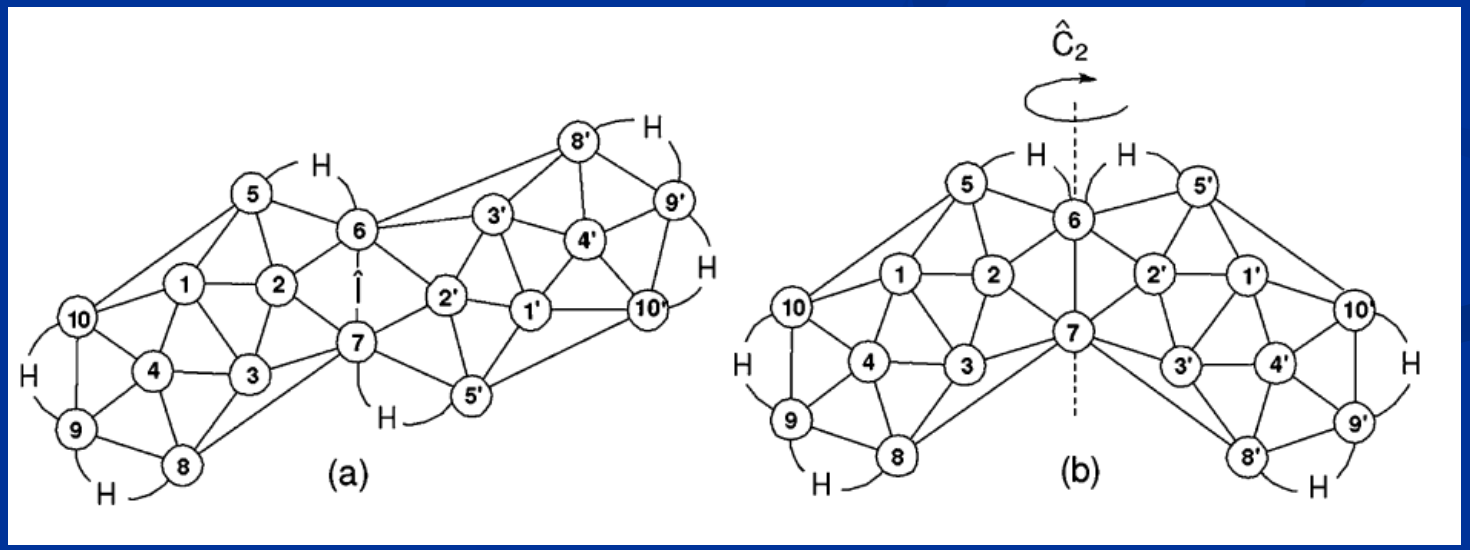

anti-$B_{18}H_{22}$ (C_i)

syn-$B_{18}H_{22}$ (C_2)

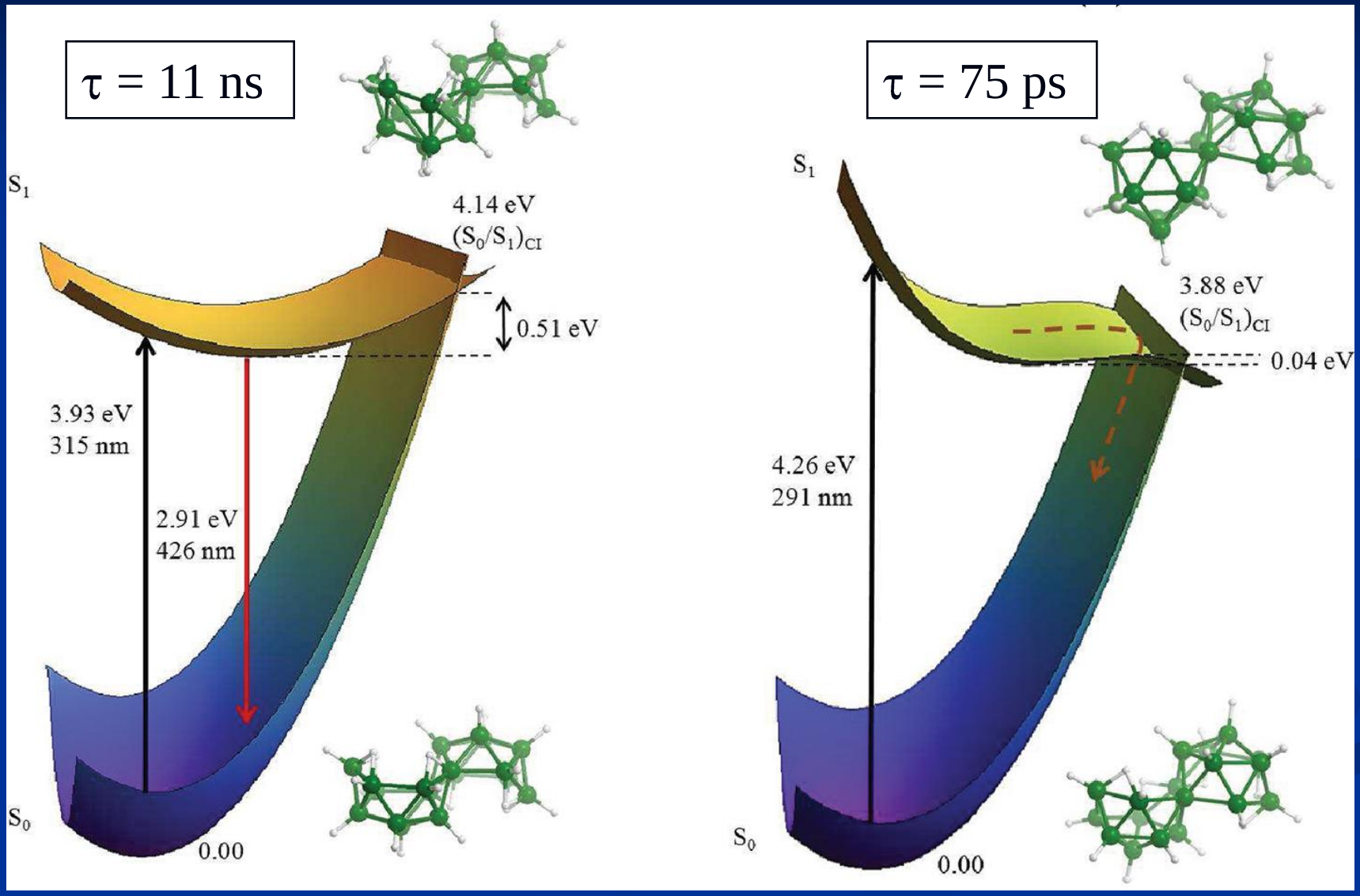

anti-$B_{18}H_{22}$ (C_i)

syn-$B_{18}H_{22}$ (C_2)

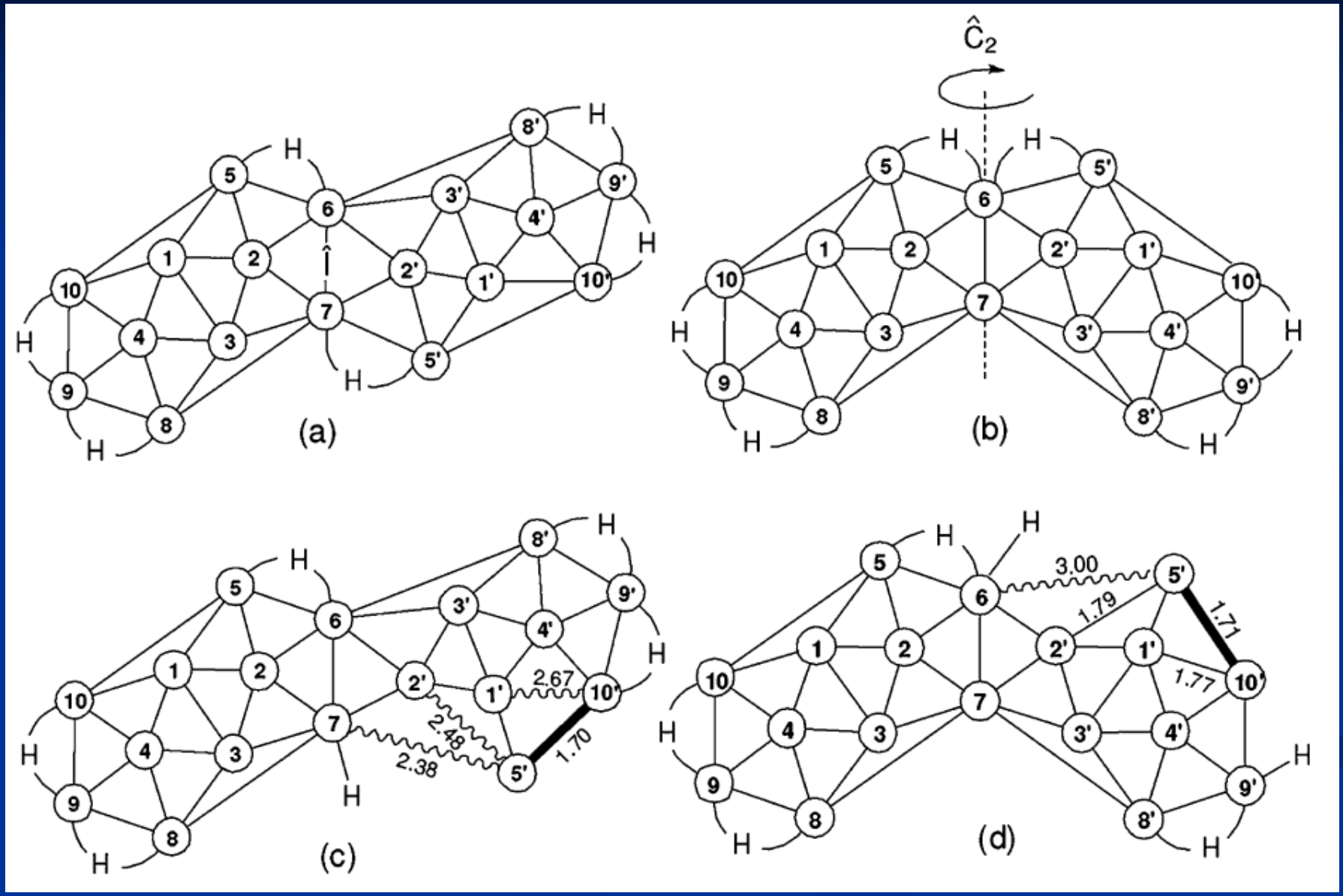

Ion-Molecule Experiments with Heteroboranes

Triple quadrupole MS/MS with Electrospray Ionization Source (ESI)

7-Tesla Fourier Transform Ion Cyclotron Resonance (7T FT-ICR)

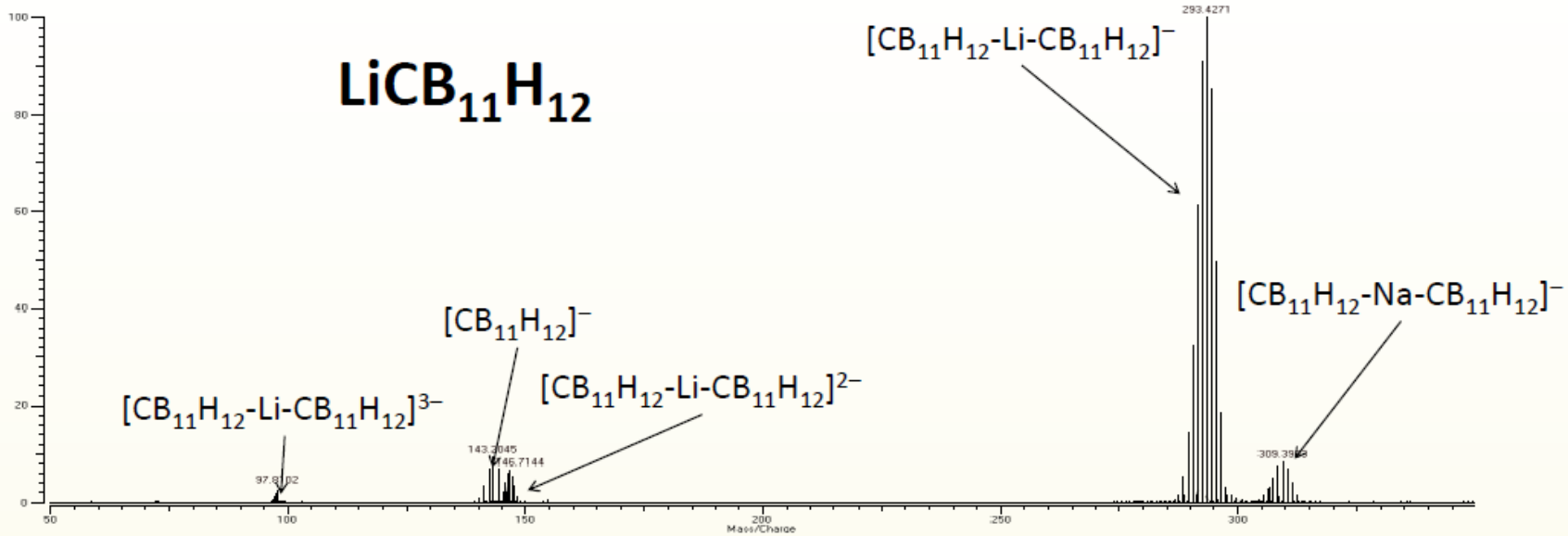

Figure 1. FT-ICR spectrum of $LiCB_{11}H_{12}$ sample, showing peaks with an isotopic mass distribution corresponding to the following anions: (a) dimer $[CB_{11}H_{12}\text{-}Li\text{-}CB_{11}H_{12}]^{3-}$; (b) monomer $[CB_{11}H_{12}]^{-}$; (c) dimer $[CB_{11}H_{12}\text{-}Li\text{-}CB_{11}H_{12}]^{2-}$; (d) dimer $[CB_{11}H_{12}\text{-}Li\text{-}CB_{11}H_{12}]^{-}$; (e) dimer $[CB_{11}H_{12}\text{-}Na\text{-}CB_{11}H_{12}]^{-}$

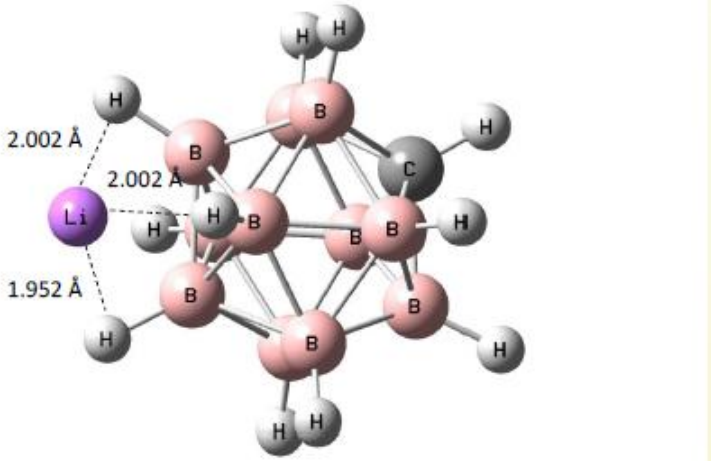

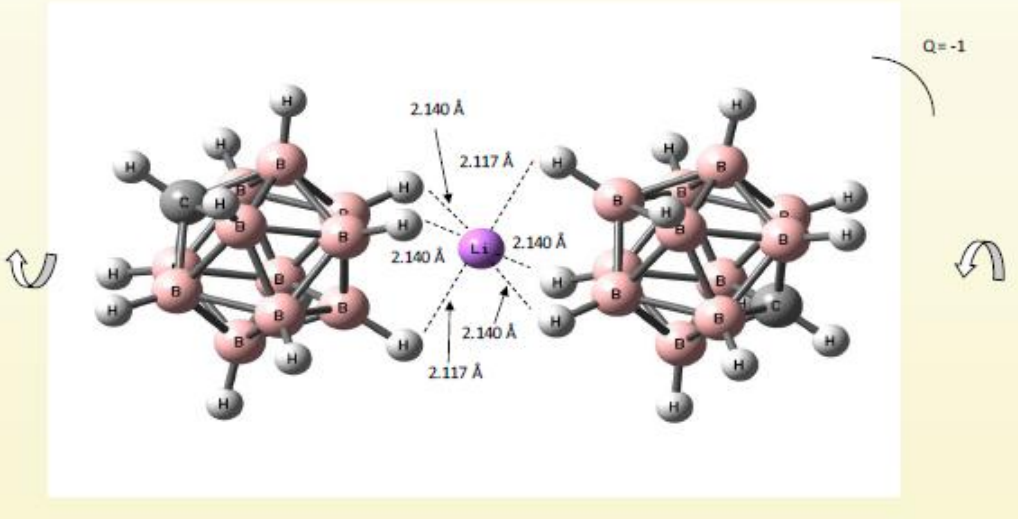

$Li_2B_{12}H_{12}$

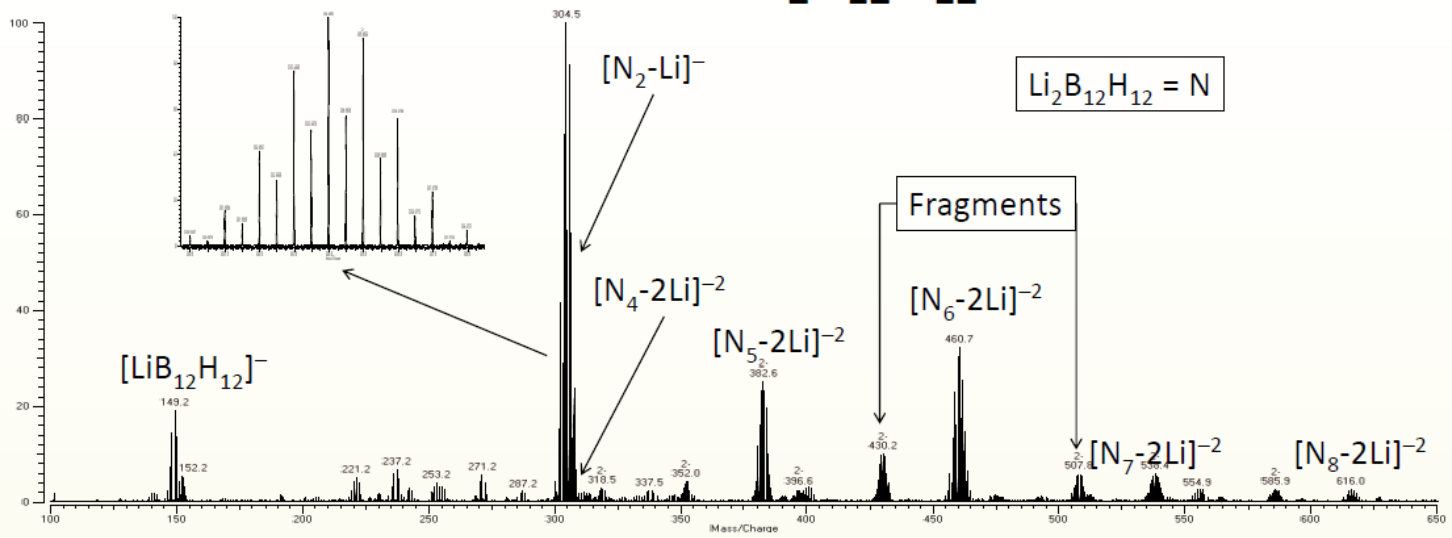

Figure 2. FT-ICR spectrum of $Li_2B_{12}H_{12}$ sample. It shows several peaks being the most intense: (a) $[LiB_{12}H_{12}]^-$ at m/z= 149.2 Da; (b) overlap of $[LiB_{12}H_{12}\text{-}Li_2B_{12}H_{12}]^-$ and $[LiB_{12}H_{12}\text{-}Li_2B_{12}H_{12}]_2^{-2}$ at m/z=304.5 Da. These peaks are very well resolved (enlargement is shown). The peaks for m/z> 370 are polymeric anions (with a charge of -2) of $[LiB_{12}H_{12}\text{-}Li_2B_{12}H_{12}]^-$ formed adding successively $Li_2B_{12}H_{12}$.

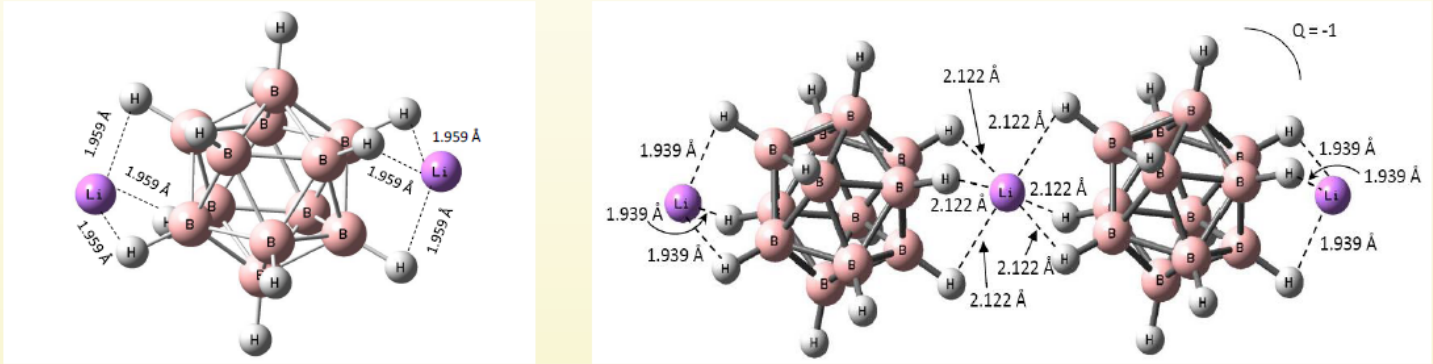

Figure 4. Optimized geometry of $(Li_2B_{12}H_{12})^-$ (left) and the most probable energy minimum for the dimer $(Li_2B_{12}H_{12})\cdots(LiB_{12}H_{12})^- \equiv [Li_{2n-1}(B_{12}H_{12})_n]^{-1}$ with n = 2 (right), calculated at the B3LYP/6-31G* level.

Boron Neutron Capture Therapy (BNCT)

$$^{10}B + n \rightarrow {}^{7}Li\ (0.84\ MeV) + {}^{4}He\ (1.47\ MeV) + \gamma\ (0.478\ MeV)$$

Natural Isotopes

^{10}B = 20%, I = 3 ^{11}B = 80%, I = 3/2

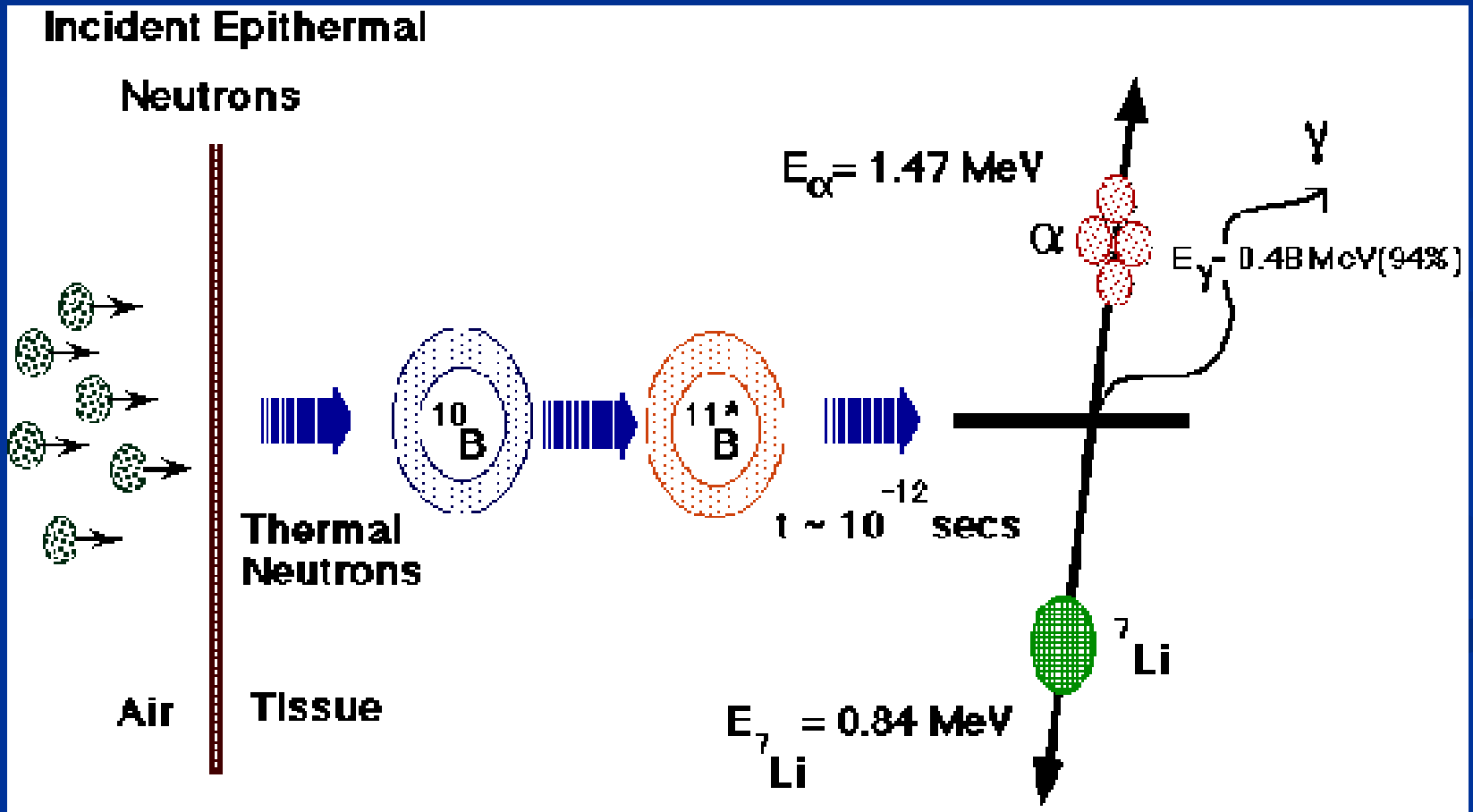

Metalaboranes inhibit HIV protease

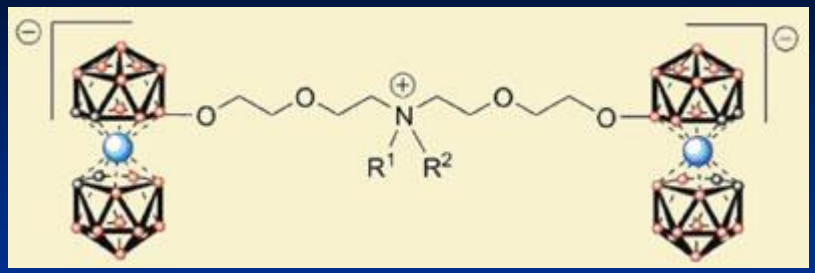

Two metallaboranes are joined by a linker chain with a central quaternary amine

X-Ray structure of the inhibitor bound to the enzime

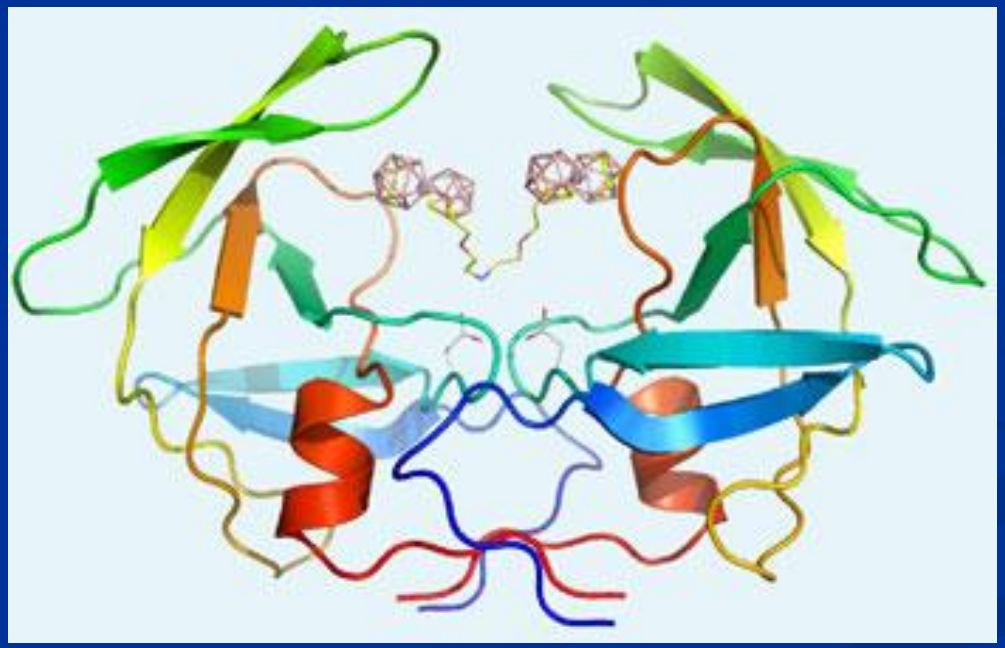

Rezácová et al, J. Med. Chem. (2009)

Valence-Bond-theoretic model Hamiltonian

$|\Phi\rangle = \phi_1(1) \quad \phi_2(2) \quad \ldots \quad \phi_N(N)$

$\langle X \rangle = \langle \Phi | X | \Phi \rangle$

Want $\mathcal{H} \equiv \Sigma_P \, \mathcal{J}_P \cdot P$ equivalent to Schrödinger H on space of $\{ P \mid \Phi > : P =$ permutation $\}$

Solution: Find $\mathcal{J}_P$ so that $< P \cdot H > = \sum_Q \mathcal{J}_Q \cdot < P \cdot Q >, \quad P \in S_N$

unique! (invert for $\mathcal{J}_P$'s)

$\mathcal{J}_P = \mathcal{J}_{P^{-1}}$ real (for standard H)

$\mathcal{J}_P$ reflect point-group & space-group symmetries

$\mathcal{J}_I \sim N^1$ *& otherwise* $\mathcal{J}_P \sim N^0$ *(or less)*

Conclusions and Future Directions

- We have explored properties on groundstate and excited state in polyhedral heteroboranes and endohedral derived systems

- Polyradical heteroborane superclusters as model systems for magnetism in 1D, 2D and 3D needs a mapping on Spin Hamiltonians or developing a VB-based Composite-System model (with Doug Klein)

$$P = P\,(\,R\,,q\,,S\,,\Psi\,)$$

- Large stability of polyhedral closed (closo) cages $\rightarrow$ ideal candidates for experimental and computational studies of soft interactions with biomolecules – role of boron in biology? (recently started research line with experimentalists)

Electronegativities: $\chi(\mathrm{C}) > \chi(\mathrm{H}) > \chi(\mathrm{B})$

Thanks

Gabriel Aullón

Moisés Canle

Juan Dávalos

Antonio Laguna

Manuela Merchán

Arturo Santaballa

Vicenta Sauri

Francesc Teixidor

Luis Serrano-Andrés†

Ángel Vegas

Clara Viñas

Diego Alcoba 

Neil Allan 

Drahomír Hnyk 

Josef Holub 

Douglas J. Klein 

Josef Michl 

Paul Schleyer 

Alan J. Welch 

Bohumír Grüner 

Thomas Schmalz 

Itai Panas